

12 LEVEL II

AD-E300811

DNA 4984F

ADA 086220

EVALUATION OF HIGH L/D EARTH PENETRATORS

AVCO Research & Systems Group
201 Lowell Street
Wilmington, Massachusetts 01887

30 November 1978

Final Report for Period 7 April 1978—30 August 1978

CONTRACT No. DNA 001-78-C-0176

APPROVED FOR PUBLIC RELEASE;
DISTRIBUTION UNLIMITED.

DDC FILE COPY.

THIS WORK SPONSORED BY THE DEFENSE NUCLEAR AGENCY
UNDER RDT&E RMSS CODE B344078464 Y99QAXSB04838 H2590D.

Prepared for
Director
DEFENSE NUCLEAR AGENCY
Washington, D. C. 20305

DTIC
ELECTE
S JUL 8 1980 D
B

80 5 19 097

Destroy this report when it is no longer needed. Do not return to sender.

PLEASE NOTIFY THE DEFENSE NUCLEAR AGENCY,
ATTN: STTI, WASHINGTON, D.C. 20305, IF
YOUR ADDRESS IS INCORRECT, IF YOU WISH TO
BE DELETED FROM THE DISTRIBUTION LIST, OR
IF THE ADDRESSEE IS NO LONGER EMPLOYED BY
YOUR ORGANIZATION.



UNCLASSIFIED

SECURITY CLASSIFICATION OF THIS PAGE (When Data Entered)

REPORT DOCUMENTATION PAGE		READ INSTRUCTIONS BEFORE COMPLETING FORM
1. REPORT NUMBER DNA 4984F	2. GOVT ACCESSION NO. AD-A086220	3. RECIPIENT'S CATALOG NUMBER
4. TITLE (and Subtitle) EVALUATION OF HIGH L/D EARTH PENETRATORS.	5. TYPE OF REPORT & PERIOD COVERED Final Report, for Period 7 Apr 78 - 30 Aug 78.	6. PERFORMING ORGANIZATION REPORT NUMBER AVSD-0127-79-RR
7. AUTHOR(s) D. Henderson	8. CONTRACT OR GRANT NUMBER(s)	9. PERFORMING ORGANIZATION NAME AND ADDRESS AVCO Research & Systems Group 201 Lowell Street Wilmington, Massachusetts 01887
10. CONTROLLING OFFICE NAME AND ADDRESS Director Defense Nuclear Agency Washington, D.C. 20305	11. REPORT DATE 30 November 1978	12. PROGRAM ELEMENT, PROJECT, TASK AREA & WORK UNIT NUMBERS Subtask Y99QXSB048-38
13. MONITORING AGENCY NAME & ADDRESS (if different from Controlling Office) 1282	14. SECURITY CLASS (of this report) UNCLASSIFIED	15. DECLASSIFICATION DOWNGRADING SCHEDULE
16. DISTRIBUTION STATEMENT (of this Report) Approved for public release; distribution unlimited.	17. DISTRIBUTION STATEMENT (of the abstract entered in Block 20, if different from Report)	18. SUPPLEMENTARY NOTES This work sponsored by the Defense Nuclear Agency under RDT&E RMSS Code B344078464 Y99QXSB04838 H2590D.
19. KEY WORDS (Continue on reverse side if necessary and identify by block number) Reverse Ballistic Tests Earth Penetrator High L/D Penetrator Off Normal Impact	20. ABSTRACT (Continue on reverse side if necessary and identify by block number) This report develops an approach for performing parametric studies of high L/D earth penetrators by using the primary response frequencies and modes. The applicability has been demonstrated by performing correlation studies of test data, detailed response analysis, and the simplified approach. The parameters that may be varied are impact velocity, angle-of-attack, tar- get material, and penetrator strength. The preliminary results are that	

DD FORM 1 JAN 73 1473 EDITION OF 1 NOV 65 IS OBSOLETE

UNCLASSIFIED

SECURITY CLASSIFICATION OF THIS PAGE (When Data Entered)

404786

LB

UNCLASSIFIED

SECURITY CLASSIFICATION OF THIS PAGE(When Data Entered)

20. ABSTRACT (Continued)

increased penetrator capability, at a given angle-of-attack, may be obtained at higher impact velocities because of the resonance phenomena.

UNCLASSIFIED

SECURITY CLASSIFICATION OF THIS PAGE(When Data Entered)

TABLE OF CONTENTS

Section	Page
1.0 Background	7
2.0 Approach and Analyses	11
3.0 Test Data Review and Correlation	19
4.0 Loading Environment	27
5.0 Correlation Studies	33
6.0 Parametric Studies	55
7.0 Conclusions and Recommendations	77
 Appendix	
A. Avco Impact and Penetration Technology Program Summary	79

ACCESSION for		
NTIS	White Section	<input checked="" type="checkbox"/>
DDC	Buff Section	<input type="checkbox"/>
UNANNOUNCED		<input type="checkbox"/>
JUSTIFICATION _____		
BY _____		
DISTRIBUTION/AVAILABILITY CODES		
Dist.	AVAIL. and/or	SPECIAL
A		

LIST OF ILLUSTRATIONS

<u>Figure</u>		<u>Page</u>
1	Penetrator design development history	8
2	Reverse ballistic (R.B.)	9
3	Representative earth penetrator (EP) configuration	13
4	Penetrator structural survival code flow diagram	18
5	P2 Half scale earth penetrator	20
6	DNA 0.284 Scale earth penetrator	21
7	Instrumented Maverick alternate warhead	22
8	Test data/prediction comparison - P2 Halfscale earth penetrator	23
9	Test data/prediction comparison - DNA 0.284 scale earth penetrator	24
10	Test data/prediction comparison - Maverick alternate warhead	25
11	2-D Code/simplified analysis loading comparison - initial version	28
12	2-D Code/simplified analysis loading comparison - final version	30
13	Axial loading comparison - P-2 Half scale earth penetrator	34
14	Lateral loading comparison - P-2 Half scale earth penetrator	35
15	Axial loading comparison - DNA 0.284 scale earth penetrator	38
16	Lateral loading comparison - DNA 0.284 scale earth penetrator	39
17	Lateral loading comparison - DNA 0.284 scale earth penetrator - Section 1	40
18	Lateral loading comparison - DNA 0.284 scale earth penetrator - Section 2	41

LIST OF ILLUSTRATIONS (Cont'd)

<u>Figure</u>		<u>Page</u>
19	Lateral loading comparison - DNA 0.284 scale earth penetrator - Section 3	42
20	Lateral loading comparison - DNA 0.284 scale earth penetrator - Section 4	43
21	Test data/analysis comparison - P-2 Half scale earth penetrator - $\alpha = 0^\circ$	44
22	Test data/analysis comparison - P-2 Half scale earth penetrator - $\alpha = 5^\circ$	45
23	Test data/analysis comparison - P-2 Half scale earth penetrator - $\alpha = 5^\circ$	46
24	Test data/analysis comparison - P-2 Half scale earth penetrator - $\alpha = 10^\circ$	47
25	Test data/analysis comparison - P-2 Half scale earth penetrator - $\alpha = 10^\circ$	48
26	Test data/analysis comparison - DNA 0.284 scale earth penetrator - S.G. 6	49
27	Test data/analysis comparison - DNA 0.284 scale earth penetrator - S.G. 3	50
28	Test data/analysis comparison - DNA 0.284 scale earth penetrator - S.G. 4	51
29	Test data/analysis comparison - DNA 0.284 scale earth penetrator - S.G. 9	52
30	Test data/analysis comparison - DNA 0.284 scale earth penetrator - S.G. 10	53
31	Parametric study results - structural material - $\epsilon_{critical} = 2\%$	56
32	Parametric study results - structural material - $\epsilon_{critical} = 4\%$	57
33	Parametric study results - structural material - $\epsilon_{critical} = 6\%$	58
34	Significance of rigid body motion on loads and response	60

LIST OF ILLUSTRATIONS (Concl'd)

<u>Figure</u>	<u>Page</u>
35 Distributed loading, $t = 100 \mu\text{sec}$	61
36 Distributed loading, $t = 500 \mu\text{sec}$	62
37 Distributed loading, $t = 800 \mu\text{sec}$	63
38 Penetrator configurations - structural ruggedness	65
39 Parametric study results - wall thickness - $\epsilon_{\text{critical}} = 2\%$	66
40 Parametric study results - wall thickness - $\epsilon_{\text{critical}} = 4\%$	67
41 Parametric study results - wall thickness - $\epsilon_{\text{critical}} = 6\%$	68
42 Penetrator configurations - L/D	70
43 Parametric study results - L/D - $\epsilon_{\text{critical}} = 2\%$	71
44 Parametric study results - L/D - $\epsilon_{\text{critical}} = 4\%$	72
45 Parametric study results - L/D - $\epsilon_{\text{critical}} = 6\%$	73
46 Penetration depth vs. wall thickness	74
47 Penetration depth vs. L/D	75

PREFACE

The main objective of this program was to develop a simplified and efficient method for performing parametric studies on high L/D earth penetrators. The approach selected showed good correlation with available experimental results and detailed analytical response data.

This program was conducted by the Avco Systems Division under Contract DNA 001-77-C-0098 for the Defense Nuclear Agency. The work was performed under the direction of Lt. Col. David R. Spangler. The Avco Program Manager for this contract was Mr. Patrick J. Grady.

The author wishes to acknowledge the contributions to the program made by Mr. J. Hollowell and Mr. E. Lawlor of the Avco Systems Division.

SUMMARY

A simplified analytical approach to a complex response problem requires the statement of several assumptions which may affect the accuracy of these results. Therefore, the simplified approach should be correlated with actual test events and existing detailed response analyses to ascertain and demonstrate the accuracy and reliability of the results.

The principal tasks conducted during this program include:

1. Review the existing test data base and detailed analytical study results.
2. Select and generate a simplified analytical approach that would be adequate to predict the necessary structural performance characteristics of a typical earth penetrator impacting and penetrating hard targets in order to determine the structural survival limits.
3. Develop computer simulation model.
4. Conduct response studies with simplified model to correlate with previous test events which have been analyzed using more sophisticated techniques.
5. Conduct parametric study of penetrator structural survival limitations.
6. Identify significant results and conclusions.

The significant results and conclusions of this study are:

1. Simplified method developed and demonstrated.
2. Effects of full body wetting proven significant.
3. Structural survival of penetrator can improve with increasing velocity and angle of attack.
4. Minimal structural survival penalty for increased payload carrying capacity.

The most significant conclusion of this study is that structural survival may be improved with increased velocity and angle of attack. This is a result of the lateral loading environment which contained a characteristic frequency dictated by the rate of body wetting or load application, which is directly related to impact velocity. The lateral response of the penetrator is also frequency dependent (i.e., the fundamental bending model). When these two frequencies are similar, a resonant condition occurs and results in the amplification of the bending stresses. Increasing the impact velocity has the effect of changing the frequency match and therefore improving the likelihood of survival in some cases.

Following a brief summary of the background to this problem, these phenomena are described in detail.

SECTION 1.0

BACKGROUND

This section presents a brief review of the efforts conducted over the past several years in support of the Impact and Penetration Technology Program. This Defense Nuclear Agency sponsored effort commenced in 1974 to establish and advance the state of the art of impact and penetration. The scope of these efforts included:

- Development of analytical tools to analyze earth penetration events for normal impact situations to establish terradynamic trajectory characteristics.
- Investigation of impact events through analysis and testing to demonstrate the community's ability to predict loading environments.
- Correlation of the subsequent analytical predictions of structural response through reverse ballistic testing.

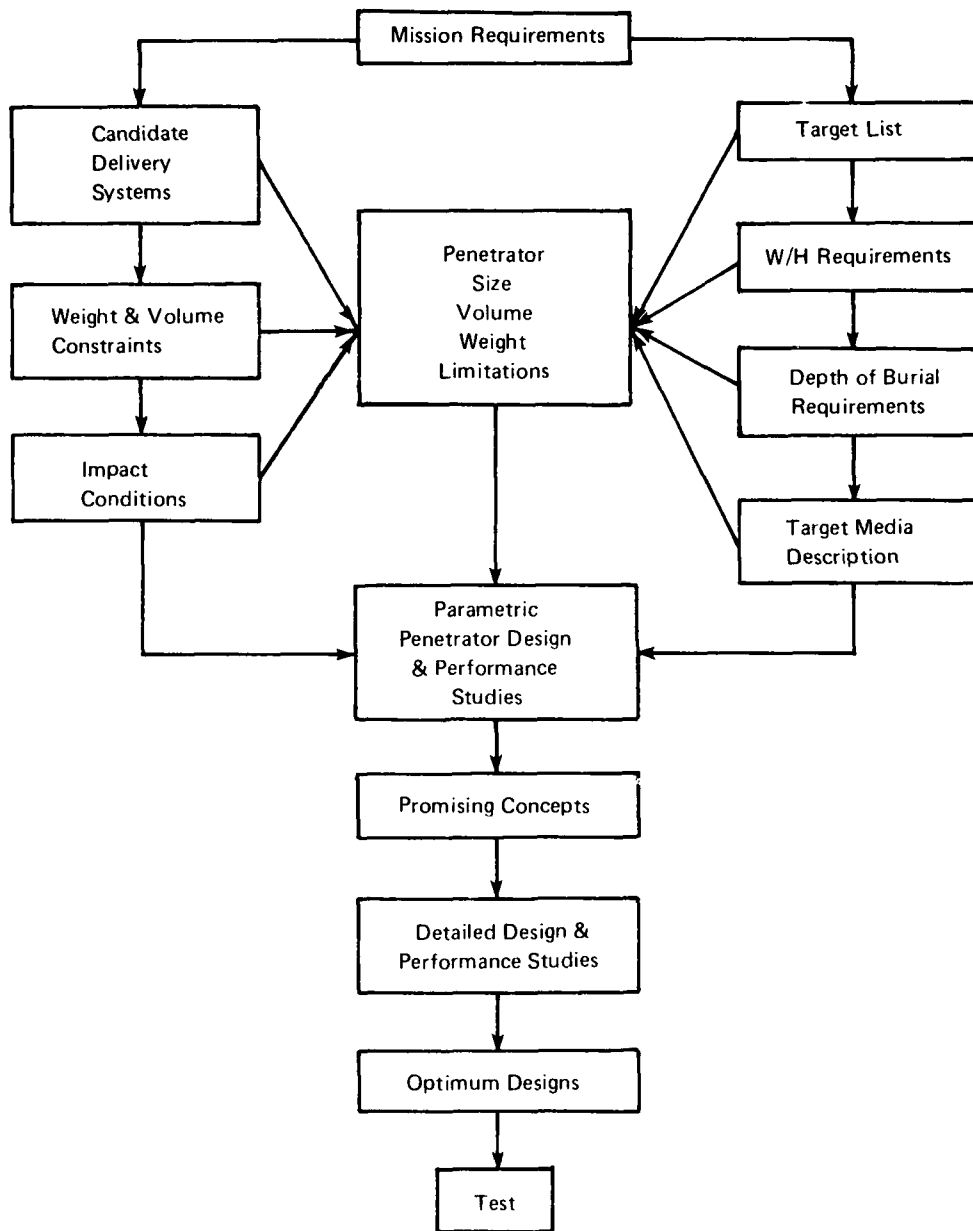
Due to program constraints the structural response effort was limited to the following parametric variations:

1. Specific designs (i.e., configuration and structural material).
2. Limited target media types.
3. Narrow range of impact velocities (1500 - 1800 ft/s).
4. Two angles of attack (0 and 3⁰) for the semi-infinite (half space) target.

Although these efforts considerably advanced the state of the art of impact and penetration it was evident that additional technology work must be accomplished to evolve an efficient earth penetrating weapon system. Figure 1 summarizes the earth penetrator design development cycle, and indicates all of the tasks that comprise the penetrator design development cycle. The efforts conducted to date by the Avco Systems Division and the other members of the penetrator community have been in the area of "Detailed Design and Performance Studies." A brief summary of the Avco Impact and Penetration Technology Program is presented in Appendix A. The principal testing technique is the reverse ballistic test (RBT) gun shown on Figure 2.

To expand this work and provide more insight for designers, the current program investigated "Parametric Penetrator Design and Performance Studies." The generation of simplified analytical models provides the tools that are required for penetrator design synthesis. As shown on Figure 1, these efforts fit into the overall penetrator design development history.

The main objective of this program was to define penetrator structural survival limitations using a first order analytical approximation. To accomplish this objective a parametric study must be conducted with the following parameters considered:



99-1342

Figure 1 Penetrator design development history



Figure 2 Reverse ballistic (R.B.)

- Impact conditions (velocity, angle of attack, etc.).
- Impact media (soft soil to rock).
- Penetrator configuration and design details (which represents unlimited variations).

The analytical tools that the penetrator community has used in the past to make predictions of specified impact events are generally not efficient and economical for parametric studies.

The following sections of this report present the Avco approaches for performing "Parametric Penetrator Design and Performance Studies."

SECTION 2.0

APPROACH AND ANALYSES

The first task of this program was to generate a simplified analytical technique which would adequately define the structural performance of a representative earth penetrator and provide an approach for performing parametric design and capability studies. These postulated goals were not necessarily compatible and it remained to be demonstrated whether or not a simplified approach would be adequate, or if more sophisticated analytical techniques were required for penetrator structural capability studies.

The extensive background of the Avco Systems Division in performing the analytical procedures and testing, provided the basis for selecting the important parameters for modeling penetrator response during impact. Some of these parameters are:

1. Adequacy of Beam theory represent the structural response of High Length to Diameter (L/D) earth penetrators. For the past 10 years Avco has applied beam theory (using primarily the lumped parameter methods) to several penetrator structural design problems and found the results to be accurate and relatively economical.
2. The principal structural response of a penetrator is made up of:
 - a. Axial response: static (or steady state) load and a superimposed vibratory induced load with a frequency corresponding to the beam model fundamental free-free axial mode.
 - b. Lateral response: a vibratory response corresponding to the beam model free-free fundamental bending mode.

Because the axial and lateral responses are orthogonal (i.e., not coupled), they can be calculated independently and the resulting axial stresses, from the axial and lateral response, can be superimposed.

If these assumptions are correct, an adequate (first order) solution can be obtained using a simple and economical approach (a modal analysis with only a few degrees of freedom). The techniques presently used, i.e., lumped parameter, finite element or finite difference, are much too complicated, expensive and time consuming for preliminary design work, and should be reserved for more detailed design studies.

2.1 PROCEDURE

The analytical approach identified by Avco encompasses the following tasks:

1. Configuration and Impact Definition

Because the simplified analytical approach is intended for parametric studies, a general method of describing the penetrator geometry and the impact

conditions is required. The relevant geometry and impact parameters for the representative high L/D earth penetrator, shown on Figure 3, are summarized below. The geometry parameters include:

l	Penetrator length
d_o	Penetrator diameter
d_i	Penetrator cavity diameter
R_g	Penetrator ogive radius
ϵ_g	Secant radius offset
S_n	Nose tip bluntness
M_1 & M_2	Concentrated masses
ρ_s	Structure density
ρ_p	Payload density (the cavity is assumed filled with a homogeneous payload)
d_c	Depth of cavity
E	Young's modulus
σ_y	Structure yield strength
ϵ_L	Allowable plastic elongation

The impact parameters of interest include:

V_i	Penetrator impact velocity
α_i	Initial angle of attack

The media descriptive parameters are described in Section 4.0.

Experience in penetrator technology has indicated that the above parameters are sufficient to describe a representative earth penetrator under typical impact conditions.

2. Loading Environment

The Avco Dynamic Force Law (ADFL) technique is used to generate the simplified analytical expressions for the loads on the penetrator during impact and penetration. In the ADFL approach loads are assumed to be uncoupled, i.e., rigid body motions are assumed to be the only significant contributions, which implies that the transient structural response does not effect the loads (not necessarily correct). Also the first attempt at generating a simplified

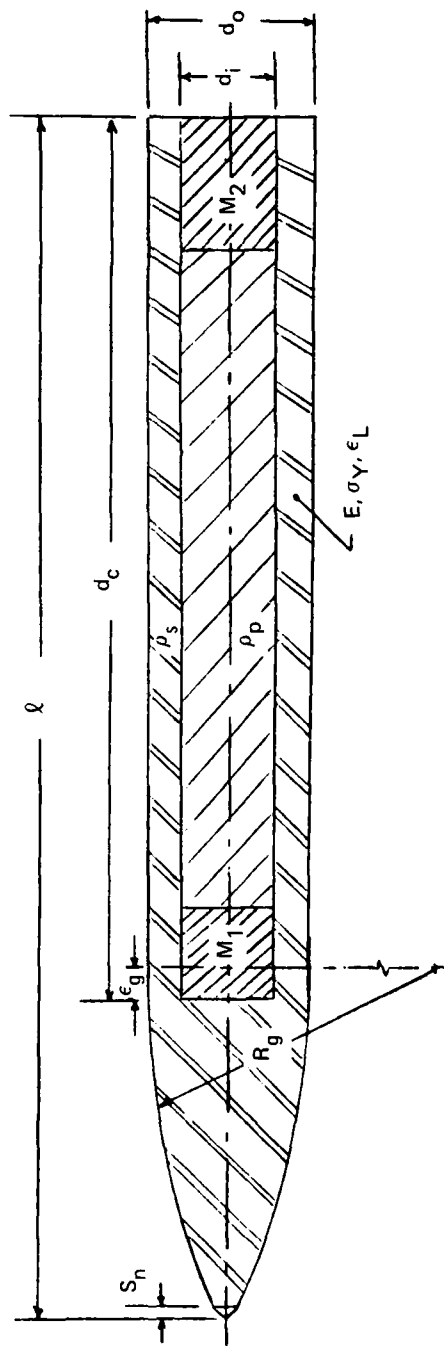


Figure 3 Representative earth penetrator (EP) configuration

99-1343

penetration simulation and specifically the loads development also assumed that the impact loads (both axial and lateral) acted only on the nose of the penetrator (nose embedment). This initial assumption proved to be inaccurate, and it was necessary in the case of the lateral loads to include fully body wetting effects, i.e., distributed loads along the length of the penetrator.

3. Axial and Lateral Mode Shapes

As a first approximation to the response mode shape a simple harmonic mode shape was assumed, i.e., half sines and cosines.

The axial mode was represented by:

$$\phi_a(x) = A + B \cos \frac{\pi X}{\ell}$$

The lateral bending mode shape was initially assumed to be:

$$\phi_b(x) = A^1 + B^1 \sin \frac{\pi X}{\ell}$$

These mode shape forms resulted in modal frequencies that were too high and therefore, a polynomial function of the form:

$$\phi_b(x) = A^1 x^2 + B^1 x^4 + C^1 x^6 + D^1$$

was then selected. This mode shape allowed the shear at the tip and tail to be zero as required, and therefore a more accurate modal frequency is obtained. The constants in the above equation were evaluated by applying the free-free boundary conditions, and, applying the actual mass distribution of the penetrator, and, finally the requirement that:

$$\int_0^{\ell} \phi_y(x) dm = 0$$

where:

$\phi_y(x)$ = the mode shape (axial or lateral)

dm = the mass distribution

ℓ = penetrator length

4. Modal Frequencies

Rayleigh's technique (Reference 3) was used to compute the fundamental axial and lateral bending modal frequencies. This method basically equates the maximum kinetic energy to the maximum potential energy of the unforced vibratory modal oscillation, i.e.,

$$K \cdot E \cdot \max = P \cdot E \cdot \max$$

or

$$T_{\max} = V_{\max}$$

For modal response, T_{\max} is proportional to the square of vibration, i.e.

$$T_{\max} = A\omega^2$$

and we can solve for the frequency of vibration,

$$\omega^2 = \frac{V_{\max}}{A}$$

the kinetic energy for both the axial and bending (lateral) modes is:

$$T_{\max} = 1/2\omega^2 \int_0^l m(x) \phi^2(x) dx$$

the potential energy for the axial mode is:

$$V_{\max} = 1/2 \int_0^l E_y \phi'(x) A_c dx$$

$$\text{where: } \phi'(x) = \frac{d(\phi(x))}{dx}$$

and for the lateral mode,

$$V_{\max} = 1/2 \int_0^l EI(x) [\phi''(x)]^2 dx$$

$$\text{where: } \phi''(x) = \frac{d^2[\phi(x)]}{dx^2}$$

Substituting the mode shapes, mass and stiffness distributions and performing the integrations numerically, results in the determination of both the axial and lateral fundamental frequencies.

5. Equations of Motion

The model equations of motion for both the axial and lateral response are:

$$M_g \ddot{\zeta} + K_g \zeta = F_g(x, t)$$

where:

- M_g = $\int \phi^2(x) M_x$ = generalized mass
- $\phi(x)$ = axial or lateral mode shape
- $M(x)$ = distributed mass of penetrator
- ζ = coordinate of model motion
- K_g = $M_g \omega^2$ = generalized stiffness parameter
- ω = axial or lateral fundamental frequency
- $F_g(y, f)$ = $\int \phi(x) F(x, t)$, the generalized forcing function
- $F(x, t)$ = the applied loading environment as a function of wetted surface area and time. (Section 4.0 describes these loads in detail.)

6. Structural Response in the Plastic Regime

In view of the fact that an earth penetrator is used only once, the structural survival design criteria should not be based on yield strength, i.e., limiting the response to the elastic regime. The design criteria should be based on the assumption that the penetrator survive, i.e., perform its intended mission. By allowing the structure to experience plastic deformation, there are generally several benefits to be gained, and these include:

- a. Weight reduction
- b. Generally available and more ductile materials can be used
- c. Fabrication costs are reduced
- d. More severe impact events can be considered
- e. Plasticity has the effect of attenuating loads to the components

It was determined that plastic deformations should be permitted and incorporated into the simplified procedure.

The equations described above provide the elastic stress/strain response, therefore the modifications to account for the effect of plastic strains are:

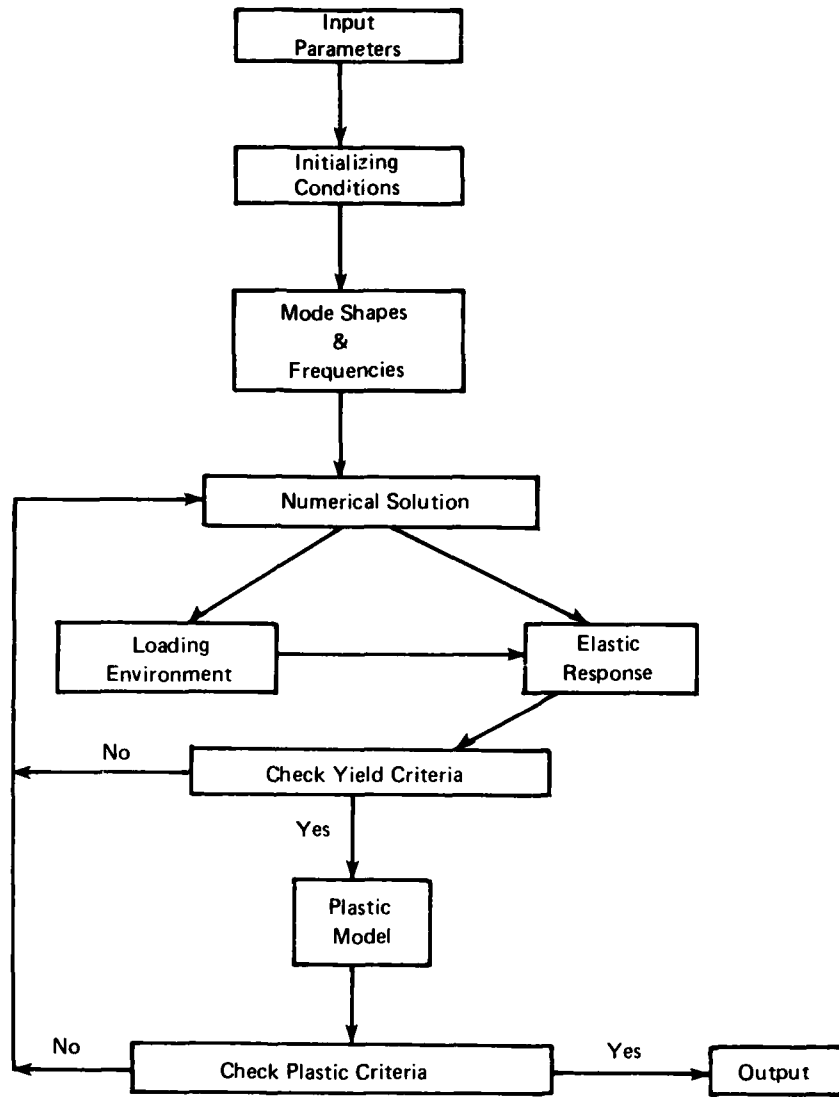
- a. Monitoring the maximum (with respect to distribution) combined (axial and lateral) elastic strains in time.
- b. Specifying a material yield strength and an allowable plastic strain.

- c. At the point in time when the deformations are allowed to continue beyond the yield point, the analytical model is modified to reflect effects of local plasticity. This was done simply by computing the local forces and deformations at the yielded location, which is then made a constant value, and continuing the dynamic solution until either a maximum deformation amplitude was achieved, or until the allowable plastic deformation (ϵ_L) was exceeded.

7. Solution of the Equations of Motion

A computer program was developed to simulate the general penetrator structural survival problem. In this computer code, the above equations of motion were programmed for the numerical solution. The code is described below and a block diagram of the subroutines is shown on Figure 4.

The input parameters consist of the penetrator geometry, material properties and impact description. The code performs several interim computations, including the penetrator mass and stiffness distributions. The numerical solution of elastic model equations of motion provides the response to the applied loads as a function of time. At each calculated time step, the loading environments and the response motion are determined. From the latter calculation and for the penetrator station with the maximum deflection, the combined yield stresses (or strains) are computed, and compared to the material yield criteria. The solution continues using either the elastic or plastic model until a maximum deformation or the plastic elongation criteria has been exceeded. The output of the computer code consists of the strain time history of the structural response.



99-1344

Figure 4 Penetrator structural survival code flow diagram

SECTION 3.0

TEST DATA REVIEW AND CORRELATION

The principal assumption upon which the simplified analytical approach is based, is that the primary or first mode is the significant contributor to the penetrator structural response. In order to check the validity of this assumption, a review and correlation of past test data was conducted. Examined in this data review were the fundamental frequency obtained from several impact experiments which were then compared to a simple lumped parameter beam theory prediction of the fundamental modal frequency.

The test data base available for review included the following:

- P-2 half scale earth penetrator (E.P.) reverse ballistic tests (FY 1975). The target media consisted of nine inches of concrete plus one inch sand in an aluminum media container. Impact velocities were on the order of 1500 ft/s with angles of attack from 0 to 10 degrees. (Reference 1)
- DNA 0.286 scale E.P. reverse ballistic tests (FY 1977). Sandstone target media impacting at 1500 ft/s, and 0 and 3 degree angles of attack (Reference 2).
- Maverick Alternate Warhead (MAW) penetrator. Tested against various concrete targets. The nominal impact velocity is 1600 ft/s and a normal obliquity test was chosen as a check on axial response.

The strain gage response data was evaluated for all of these tests. A sketch of all of these instrumented penetrators is shown on Figures 5, 6 and 7.

Prior to the above test program a pretest prediction of the structural response was made. The pretest analyses consisted of detailed loading history calculated with the Avco 2-D Impact and Penetration computer code and then a lumped parameter structural response analysis. Some of the correlation of the predictions and test results are shown on Figures 8, 9 and 10. The excellent agreement is indicative of the accuracy with which predictions can be made using this type of analysis.

To generate a simplified structural response analysis procedure, the principal assumption that the fundamental mode was dominant in the response had to be verified. Because the lumped parameter analysis method is based on beam theory, the structural response predicted consists primarily of fundamental mode response. This is also evident from the close agreement found between test data and analytical predictions. A detailed study of all of the test data response indicates that the contributions of the higher response frequencies is less than 10 percent of the total response.

The test data review provided the following conclusions: (1) Treating E.P.'s structurally via beam theory is a valid approach. (2) First mode response is the primary element of structural response. Thus the simplified analytical procedure has been verified.

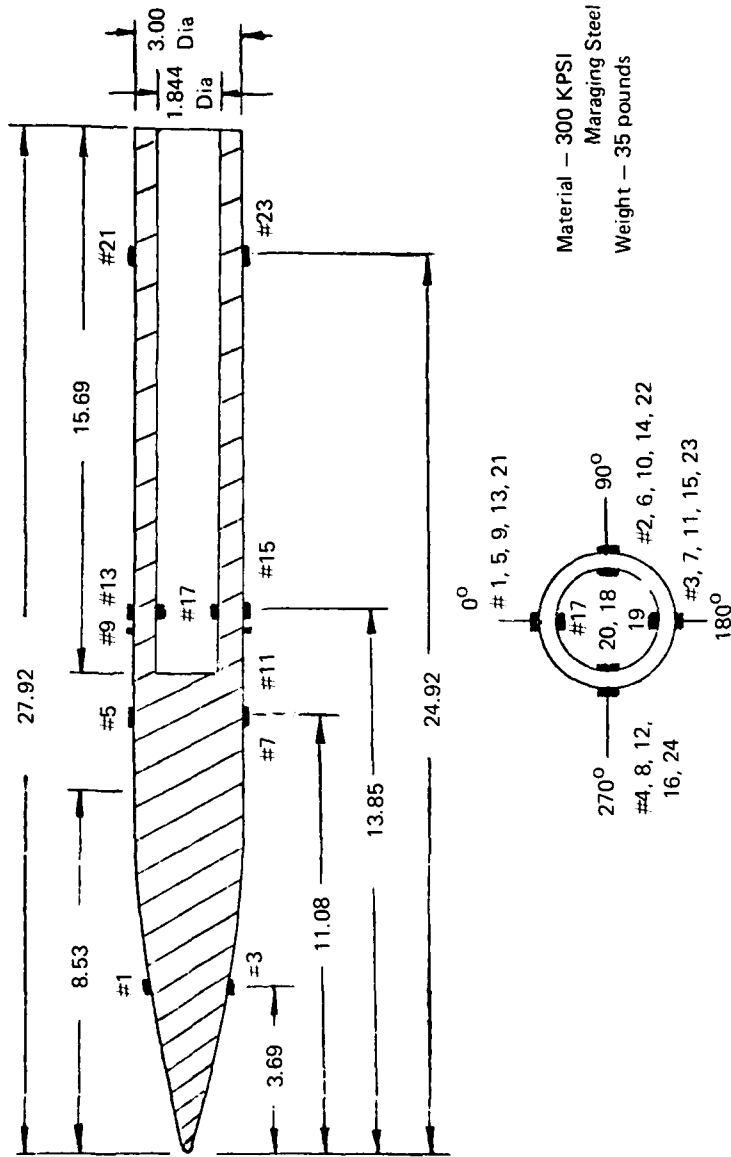


Figure 5 P2 Half scale earth penetrator

99-1345

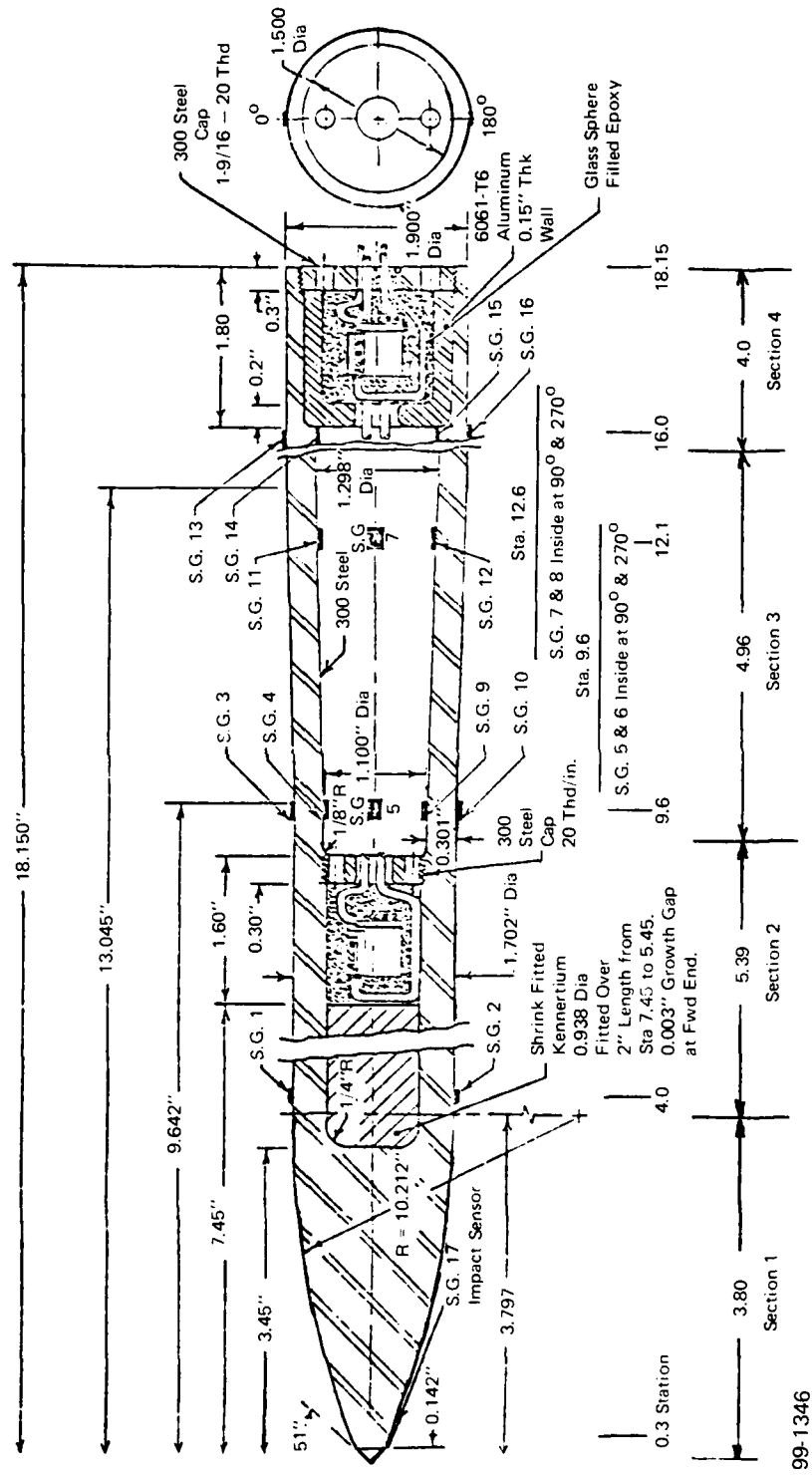
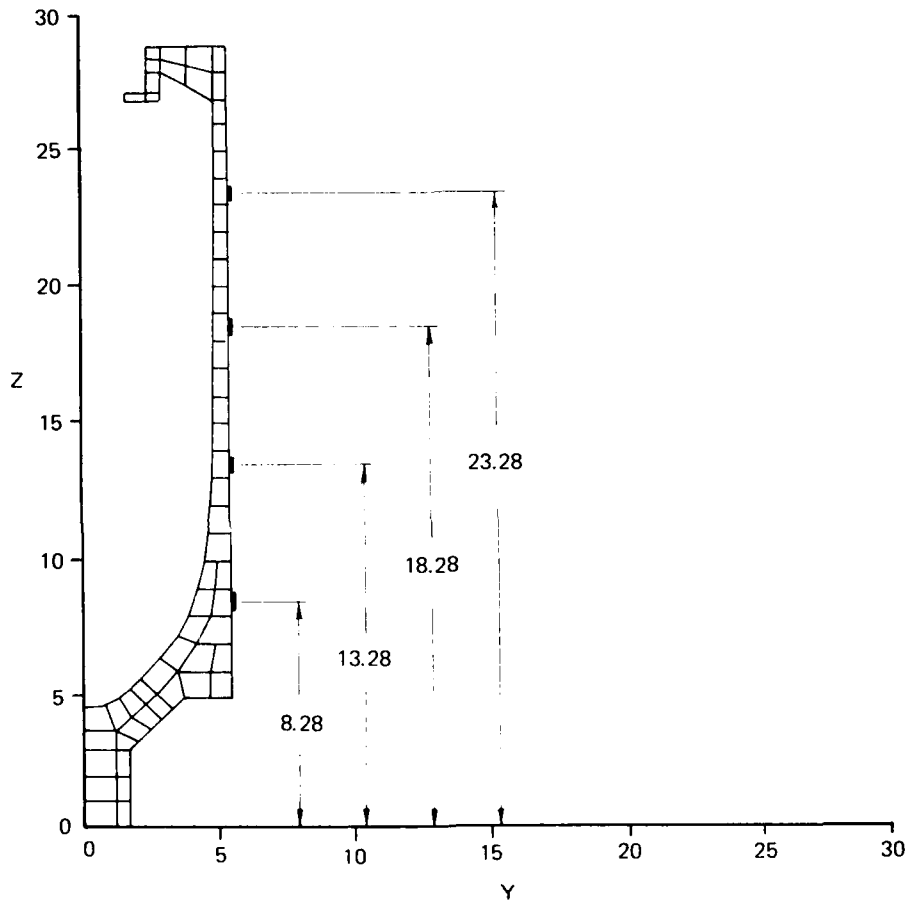
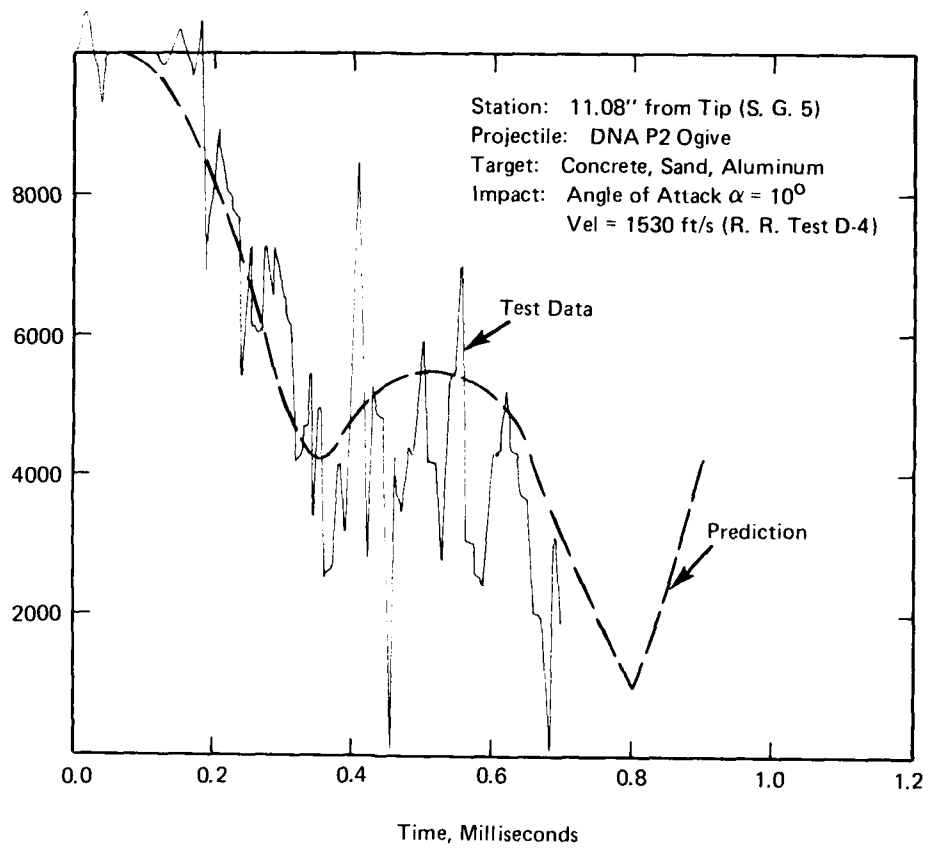


Figure 6 DNA 0.284 Scale earth penetrator



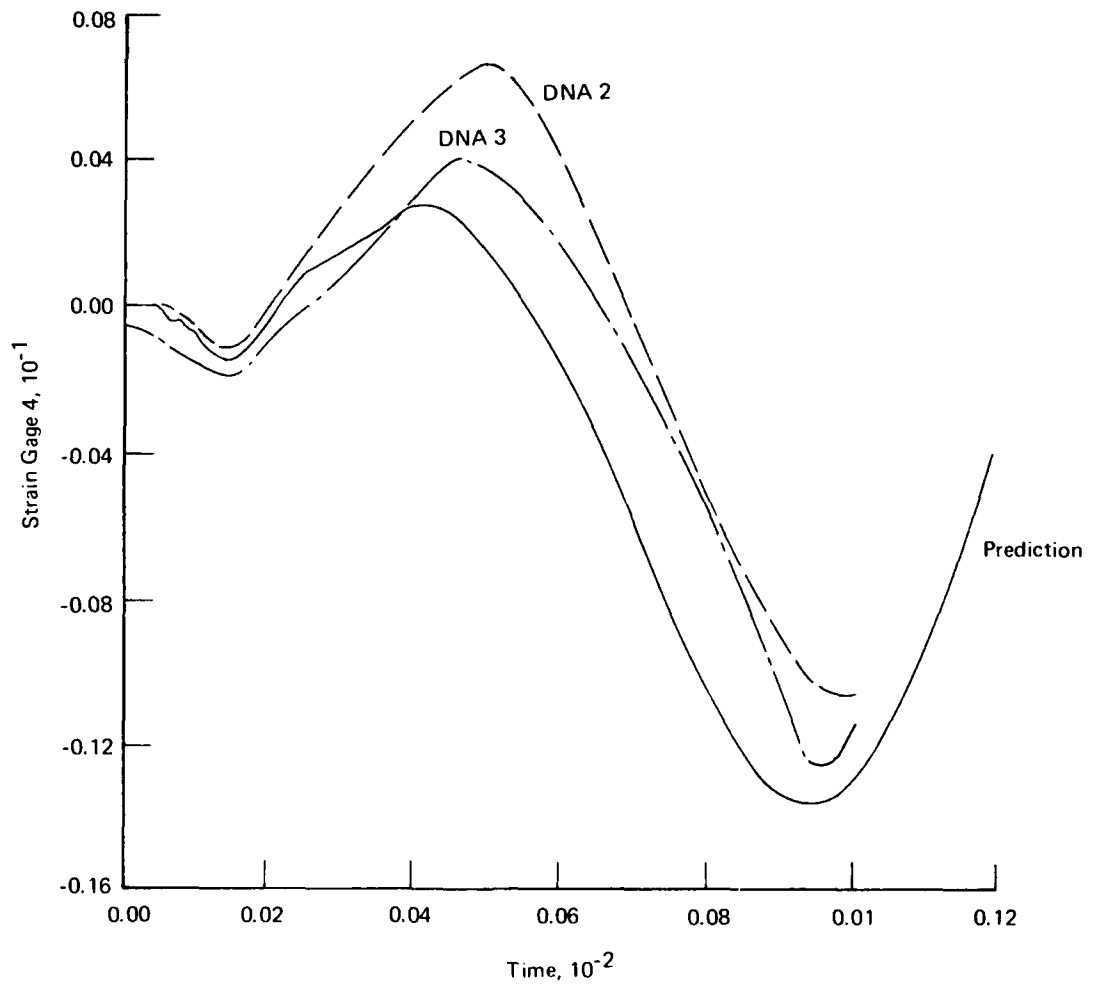
99-1347

Figure 7 Instrumented Maverick alternate warhead



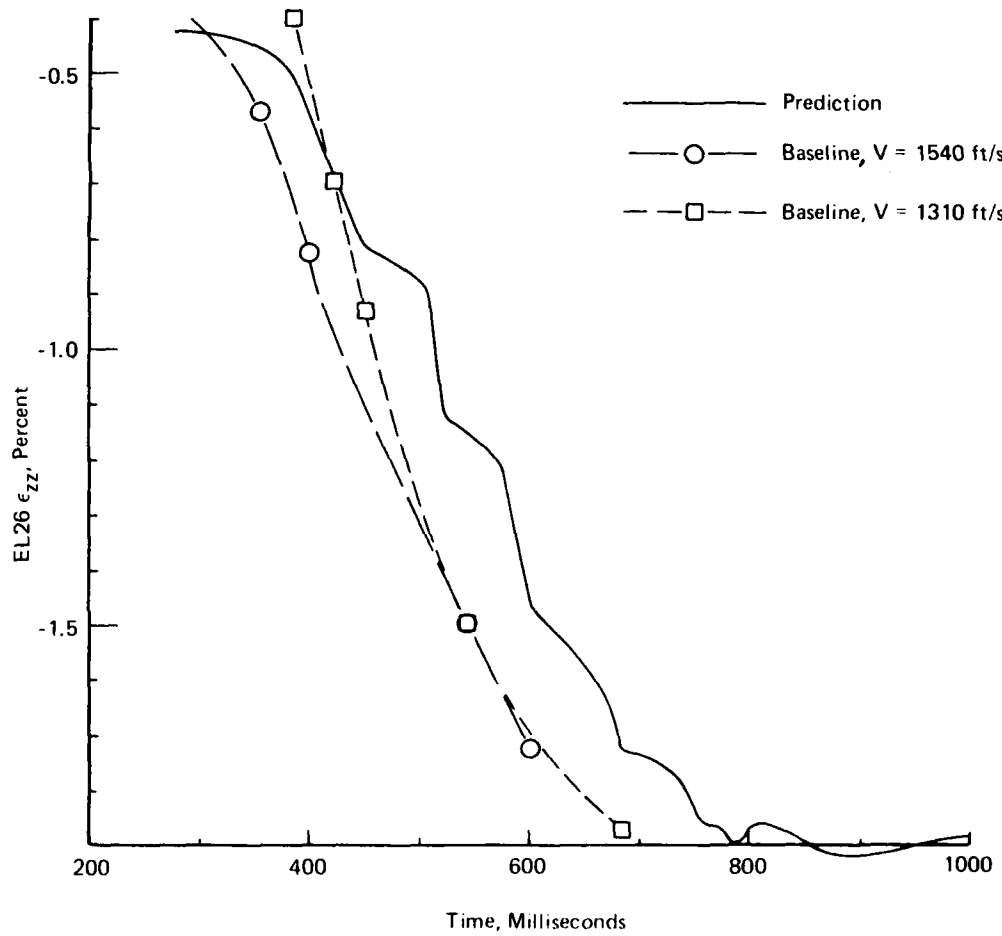
99-1348

Figure 8 Test data/prediction comparison — P2 Half scale earth penetrator



99-1349

Figure 9 Test data/prediction comparison – DNA 0.284 scale earth penetrator



99-1350

Figure 10 Test data/prediction comparison – Maverick alternate warhead

SECTION 4.0

LOADING ENVIRONMENT

The determination of the impact loading environments and the simulation of the general (rigid body) impact and penetration event is based on the Avco Impact and Penetration 2 and 3-Dimensional Computer Codes. The analytical techniques employed are a differential force law and a system of target media classification based on various physical characteristics of the media. This approach provides the basis for the classification of many different target media ranging from loosely packed sand to concrete and steel. Previous analytical and experimental correlation studies indicate that this technique is accurate for predicting penetration trajectories and also reasonably accurate in determining the loading environments during impact and penetration. The latter results, when coupled with a lumped parameter analysis, provide an accurate prediction of the structural response of the penetrator.

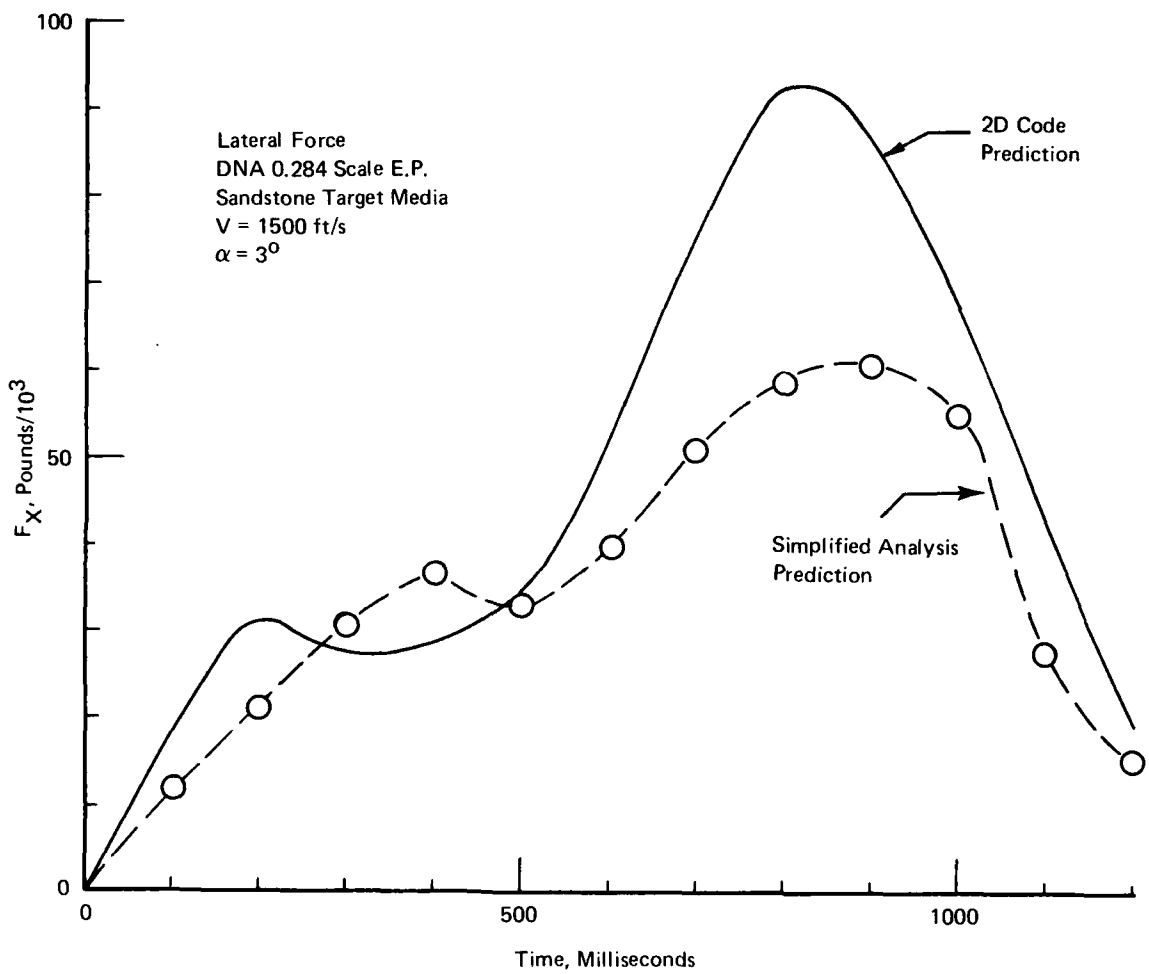
The approach taken in developing the loading environment was to modify the Avco (2-D) code in order to reduce the computational time, but still maintain a reasonable degree of accuracy. The model for the 2-D code considers the earth penetrator (E.P.) as several discrete elements. The loads are calculated for each of these elements using the differential force law and the resulting distributed loads are then integrated to provide the total loading environment. The rigid body motion of the E.P. is controlled by the loading environments.

The assumptions made for the first iteration in the loading environment determination are:

- Single target media, normal obliquity, with angle of attack.
- Nose loading is of primary importance.
- The E.P. can be treated as an element with axial and lateral loading applied to the nose.
- Rotational rigid body response motion does not greatly effect the subsequent loading environment.

Both the axial and lateral loading was applied to a location on the penetrator, two-thirds of the length from the nosetip. The peak loading occurred at full nose wetting and then attenuated as a function of the E.P. velocity decay. The application of this procedure indicated good agreement for the axial loading, but the lateral loading was significantly in error. This is evident on Figure 11 which shows the lateral loading produced from a reverse ballistic sled test at $\alpha = 30^\circ$ and is compared with the 2-D code prediction.

The 2-D code prediction showed that for full body penetration events significant lateral loading occurs along the entire E.P. body. Thus, the



99-1351

Figure 11 2-D Code/simplified analysis loading comparison — initial version

assumption that nose loading governs the event is true only during nose wetting. In addition, rigid body motion, particularly pitching motion, can significantly alter subsequent lateral loading. In the axial direction, the assumption of nose loading only holds true since at the time of full nose wetting the total axial cross-sectional area is encountered and further increases in the loading do not occur.

In the lateral response case, these results led to a second iteration in the generation of a simplified loading environment analysis procedure. The assumptions made for the revised loading model are:

- Single target media, normal obliquity, with angle of attack.
- Axial loading reaches peak at approximately full nose wetting. Subsequent decay resulting from velocity reduction.
- Lateral loading is applied on four sections of the E.P.
- Level and direction of lateral loading in all four sections based on local cone angle, angle of attack, and instantaneous lateral motion.
- Rigid body motion is fed back into axial and lateral loading calculations.

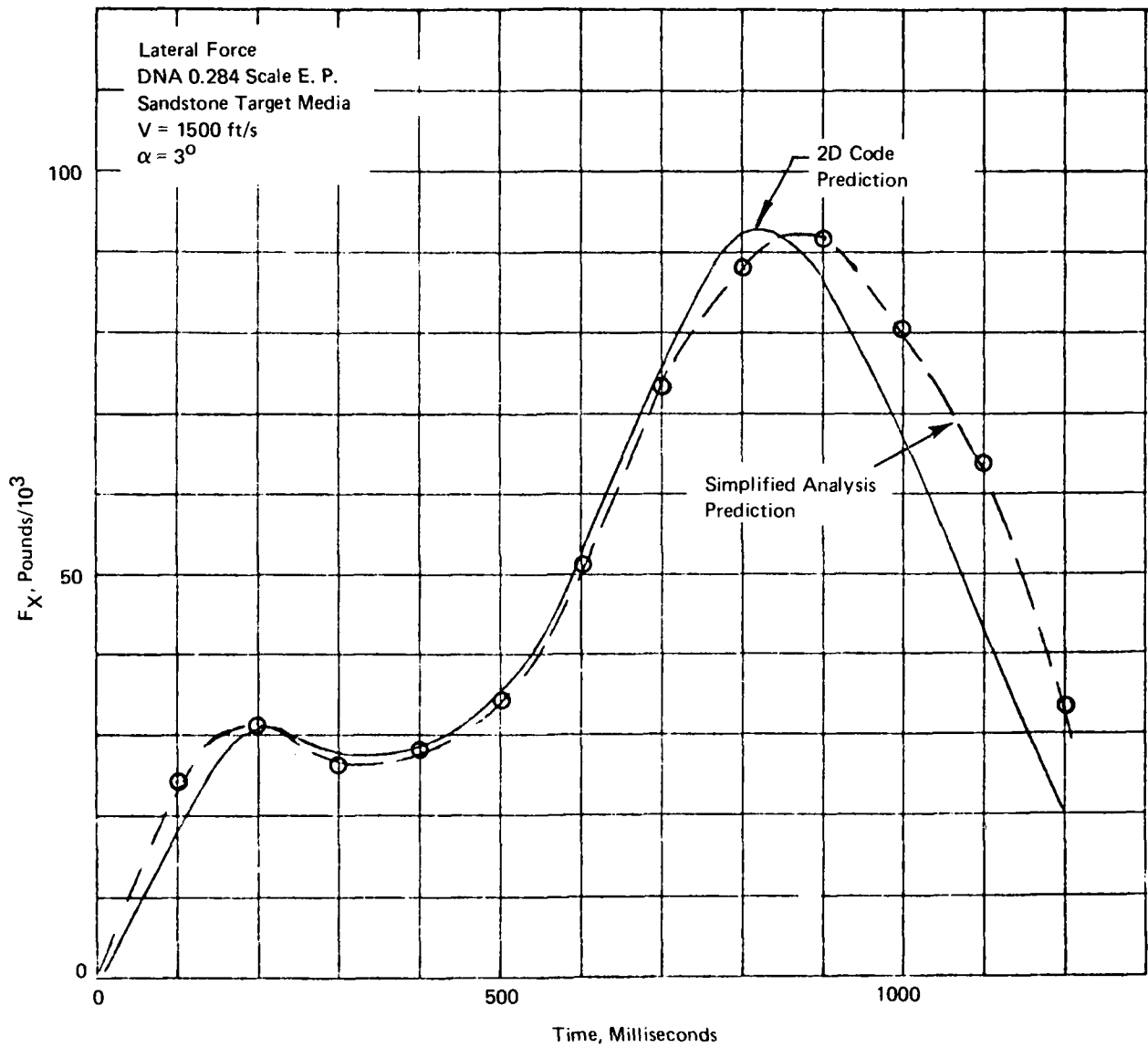
These assumptions were included into the analytical loads determination and the sandstone impact event was again simulated. A comparison of the lateral loading environment calculated from the simplified analysis and the 2-D code prediction are shown on Figure 12 and it is apparent that this procedure yields excellent agreement.

The final form of the force law is presented below:

$$F_{AXIAL} = \left[\eta \left(1 + f_c \frac{\cos \theta_c}{\sin \theta_c} \right) + \frac{1}{2} \rho v^2 (C_D \sin^2 \theta_c + C_T \cos^2 \theta_c) \right] \sin \theta_c A_c$$

$$F_{LATERAL} = \sum_{iel}^4 f_{LATERAL}(i)$$

$$f_{LATERAL} = \left[\left(\eta + \frac{1}{2} \rho C_D v^2 \sin (\theta_c + \alpha) \right) \sin (\theta_c + \alpha) - \left(\eta + \frac{1}{2} \rho C_D v^2 \sin (\theta_c - \alpha) \right) \sin (\theta_c - \alpha) \right] A_{c_L}(i) \quad (0.8)$$



99-1352

Figure 12 2-D Code/simplified analysis loading comparison — final version

where:

$\eta, f_c, \rho, C_D, C_T$ - are media dependent variables describing respectively; resistance to penetration, friction coefficient, density, normal and tangential accommodation coefficients.

V - local velocity magnitude

θ_c - local cone angle

α - local angle of attack

A_c - axial cross-sectional area

$A_{cL}(i)$ - lateral cross-sectional area

The axial loading is applied at the midpoint of the nose section and the individual lateral loadings are applied at the midpoints of their respective sections. The total loading of an element is treated as a ratio of the wetted area to the full wetted area. The local velocity and angle of attack is calculated from the rigid body motion and the distance from the penetrator c.g. to the sectional midpoints. For the nose section, the cone angle is assumed to be approximately:

$$\theta_{enose} = \tan^{-1} \left(1.2 \frac{R}{L_N} \right)$$

where:

R = E.P. radius

L_N = nose length

The axial force and distribution of lateral loading are used to determine the rigid body motion.

This procedure and the assumptions upon which it is based provide a simple, fast, and reasonably accurate method of loading environment determination. The following section will show in more detail the potential of this simplified analysis technique to predict loading environments and structural response in several example cases.

SECTION 5.0

CORRELATION STUDIES

In order to demonstrate the capability of this simplified approach to predict structural response, two test conditions were simulated. The tests selected for this correlation study are:

Case 1 Avco reverse ballistic tests.

$V = 1500 \text{ ft/s}$, $\alpha = 5^\circ, 10^\circ$ (Reference 1)

Case 2 Avco/Sandia reverse ballistic sled test.

$V = 1500 \text{ ft/s}$, $\alpha = 3^\circ$ (Reference 2)

These tests were selected since they provide a check on both the axial and lateral response prediction capabilities.

A two step procedure was initiated to check the accuracy of the simplified analysis procedure. The two steps are: 1) a comparison of the generated loading environments and 2) a comparison of the subsequent structural response. In the first case, the loading environments from the simplified procedure were compared against the 2-D Impact and Penetration computer code prediction. In the second case, the structural response was compared with both strain gage data from the tests, and detailed lumped parameter response predictions based on the 2-D code loading environments. It was shown in the preceding section that the 2-D code/lumped parameter analytical results correlate closely with the test data.

The penetrator geometries for the two tests described above are shown on Figures 5 and 6. In the case of the P2 half scale E.P. (Reference 1) only 3.6 inches of the nose portion was assumed to be loaded. This assumption was based on the effective size of the concrete media, for which both test data and 2-D code analysis indicated that load relief occurred at this depth of penetration. In addition, only the first 560 μsec of the event is valid because of subsequent impact with the aluminum media container. (See Reference 1 for details.) In the case of the DNA 0.284 scale E.P. (Reference 2) full body penetration was experienced. Thus, the analytical model for these two tests was generated with the following two assumptions: 1) the projectile is modeled in four sections, and 2) because of the limitations in the modeling procedure, the aft flare was not considered.

Figures 13 and 14 present comparisons between the 2-D code and simplified analysis for Case 1 (half scale P2) reverse ballistic test loading environments. The axial loading environment shown in Figure 13 agrees reasonably well with the 2-D code prediction. The simplified analytical prediction appears somewhat higher than the 2-D code prediction, which is due to a combination of factors including linear extrapolation of the nose loading and significant

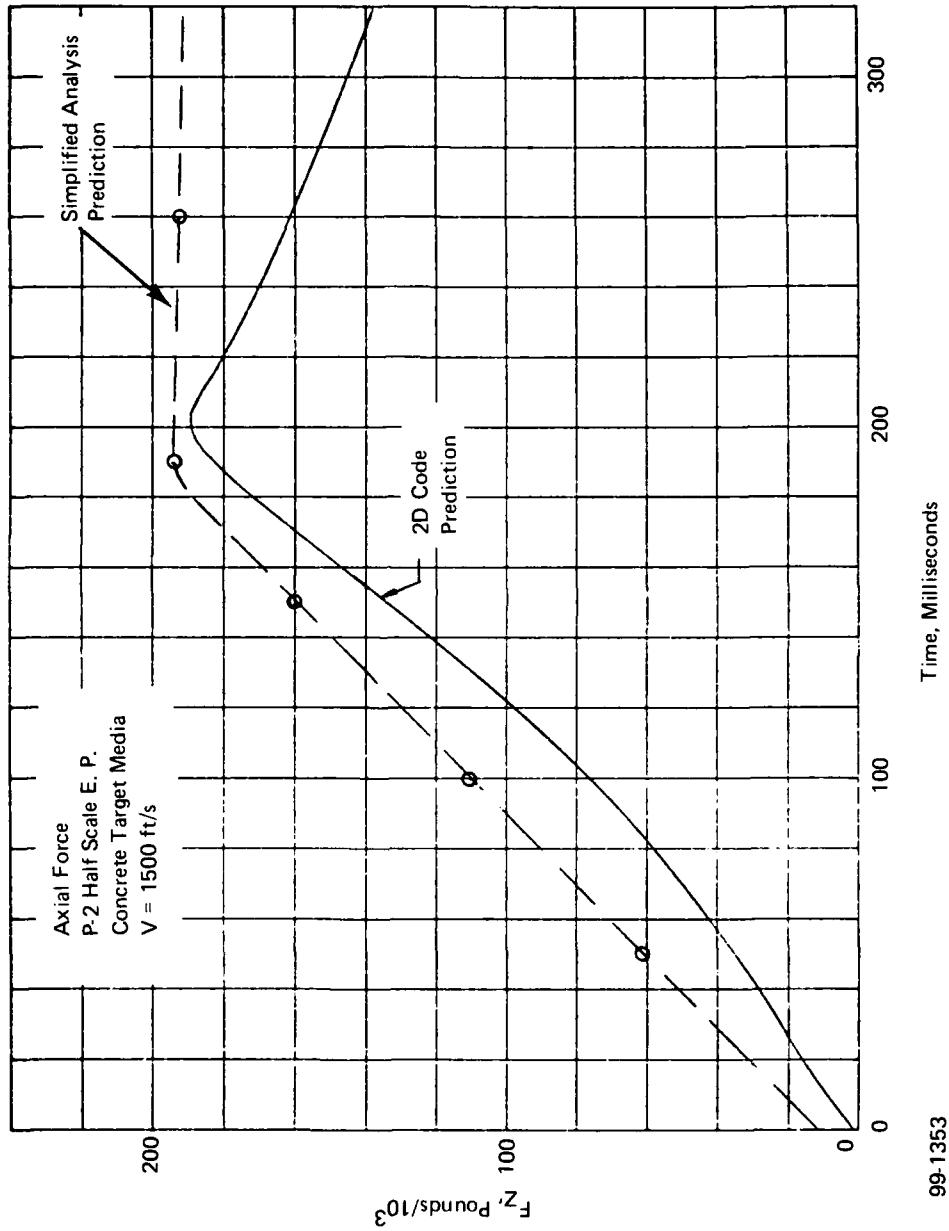


Figure 13 Axial loading comparison - P2 Half scale earth penetrator

99-1353

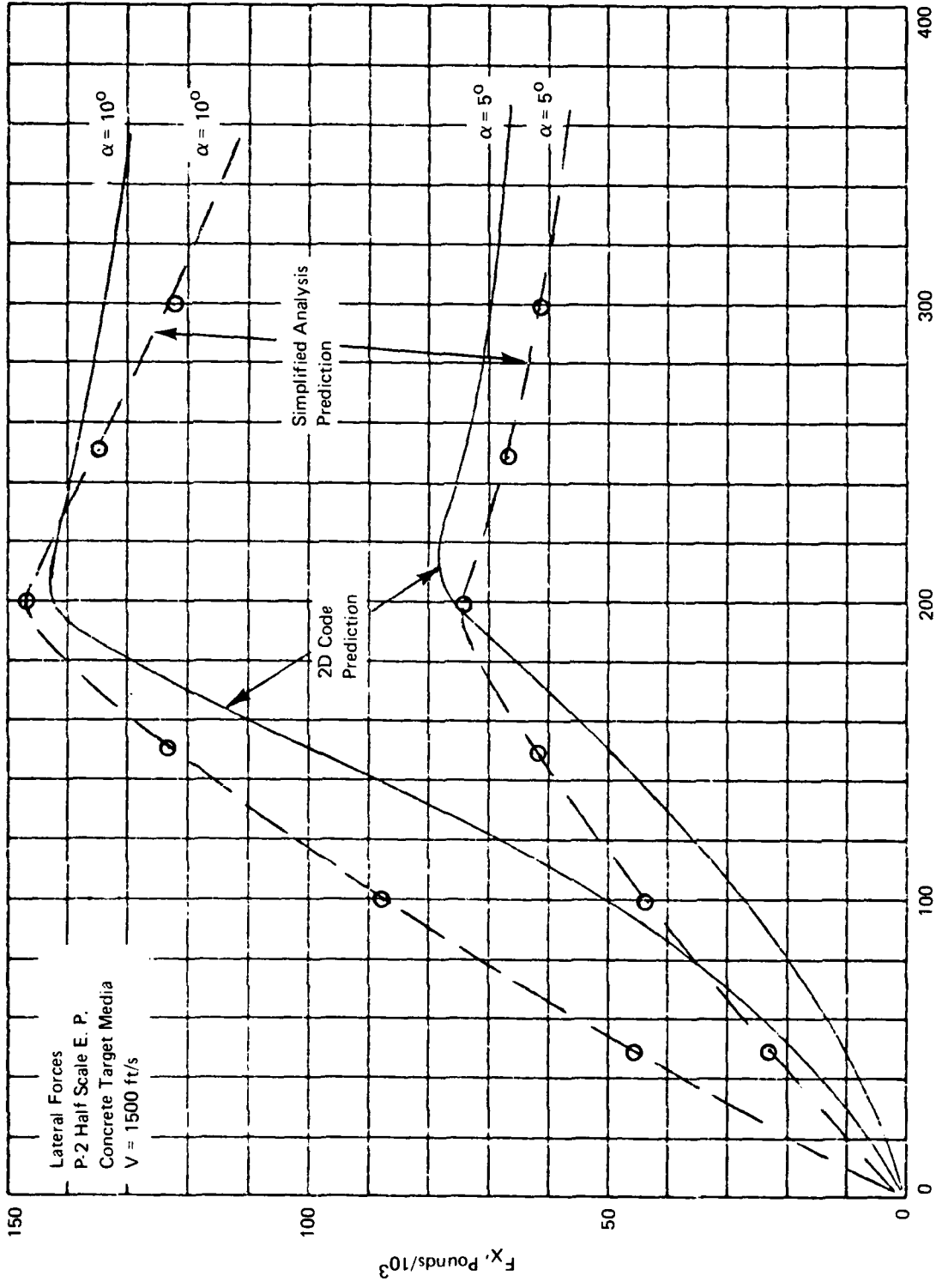


Figure 14 Lateral loading comparison - P-2 Half scale earth penetrator

99-1354

concrete load relief experienced in the actual test caused by stress wave reflections from the limited target size. The simplified analytical predictions start at a non-zero loading due to modeling of the relatively blunt nosetip. For the lateral loading environment, shown on Figure 14, the same general trends appear as in the axial loading environment. In summary, there is good agreement in both shape and phasing, with variations in amplitude being attributed to the complexity of the impact event.

The Case 2 (DNA 0.284 scale) sled test loading environment comparisons between the 2-D code and simplified model are presented in Figures 15 through 20. On Figures 15 and 16 are shown the total axial and total lateral forces, respectively. And on Figures 17 through 20 the lateral loading on each of the four individual model sections are compared. In all cases excellent agreement between the 2-D code and the simplified model is found through full penetrator body wetting (i.e., ~ 1200 μ sec).

These comparisons demonstrate that the simplifying assumptions used in this new analytical procedure provide excellent correlation with the 2-D code. In addition, because of the simplicity of this new procedure, loading environments can be generated in a fraction of the time that was required for more detailed 2-D code.

The ultimate correlation of the simplified analytical procedure is the comparison of the structural response predictions with the detailed lumped parameter analytical predictions based on the 2-D code loading environments and the experimental data.

The strain response histories for Case 1 (half scale P2) are shown on Figures 21 through 25 for angles of attack from 0° to 10° . These figures show both the axial and combined axial/bending responses. On Figure 21 for $\alpha = 0^\circ$, the axial response calculated from the simplified procedure exhibits a somewhat faster rise time than the test data or lumped parameter prediction. Also the response after 3.6 inches of nose penetration does not decay as much. In general the agreement is quite good in predicting the amplitude of the first strain peak and the overall shape of the response. The differences can be attributed to the simplifying assumptions in modeling of the impact event, as discussed previously. It should also be noted that because of the scope of this study only an approximation of the true projectile mode shape was used, and is another source of error.

The 5 and 10 degrees angle of attack combined axial/bending responses are shown on Figures 22, 23, 24, and 25. The agreement between experimental results and the lumped parameter predictions is considered good. Again the differences in frequency, phase shift, amplitude and late time response are attributed to the factors described previously, but the differences are relatively minor.

Structural response comparisons for the Case 2 reverse ballistic sled tests are presented in Figures 26 through 30. For the axial response, Tests 1 and 3 (Reference 2) at $\alpha = 3^\circ$ are used in this comparison.

The axial response is compared in Figure 26 and shows good agreement in timing and shape of the simplified analysis, detailed lumped parameter analysis and experimental data. The simplified analysis produces a conservative, higher level of response which is attributed to the assumption of neglecting the aft flare from the simplified penetrator model. The 5 and 10 degrees angle of attack strain combined response is shown in Figures 27 through 30 for both the internal and external mounted (Reference 2) strain gages. In the simplified analytical approach the external strains were calculated. The reason for showing both internal and external strain gage response is due to the limited strain data obtained at these strain gage locations. Looking at the external strain gages, 3 and 10, shown on Figures 27 and 30, respectively, it is evident that the simplified procedure is in good agreement with the more detailed lumped parameter model and with the existing experimental data. The major differences in agreement occur in the timing and level of the reverse peak. The smaller amplitude and late timing of the simplified analysis approach is attributed to the inaccuracies in the mode shape and primary frequency assumed for the projectile. It should be noted that for completeness both the elastic and plastic responses are presented on the figures, and the plastic regime analysis provides the best agreement with test data and lumped parameter predictions.* It is thought that a further refinement of the mode shape and frequency would lead to an even better correlation.

These detailed correlation studies have demonstrated the credibility of the simplified analytical approach. The source of minor discrepancies in the predictions is believed to be understood and with a minimum of refinement in assumed mode shapes and frequencies, the prediction capability of this technique would achieve an even better level of accuracy.

*Based on linear elastic analysis.

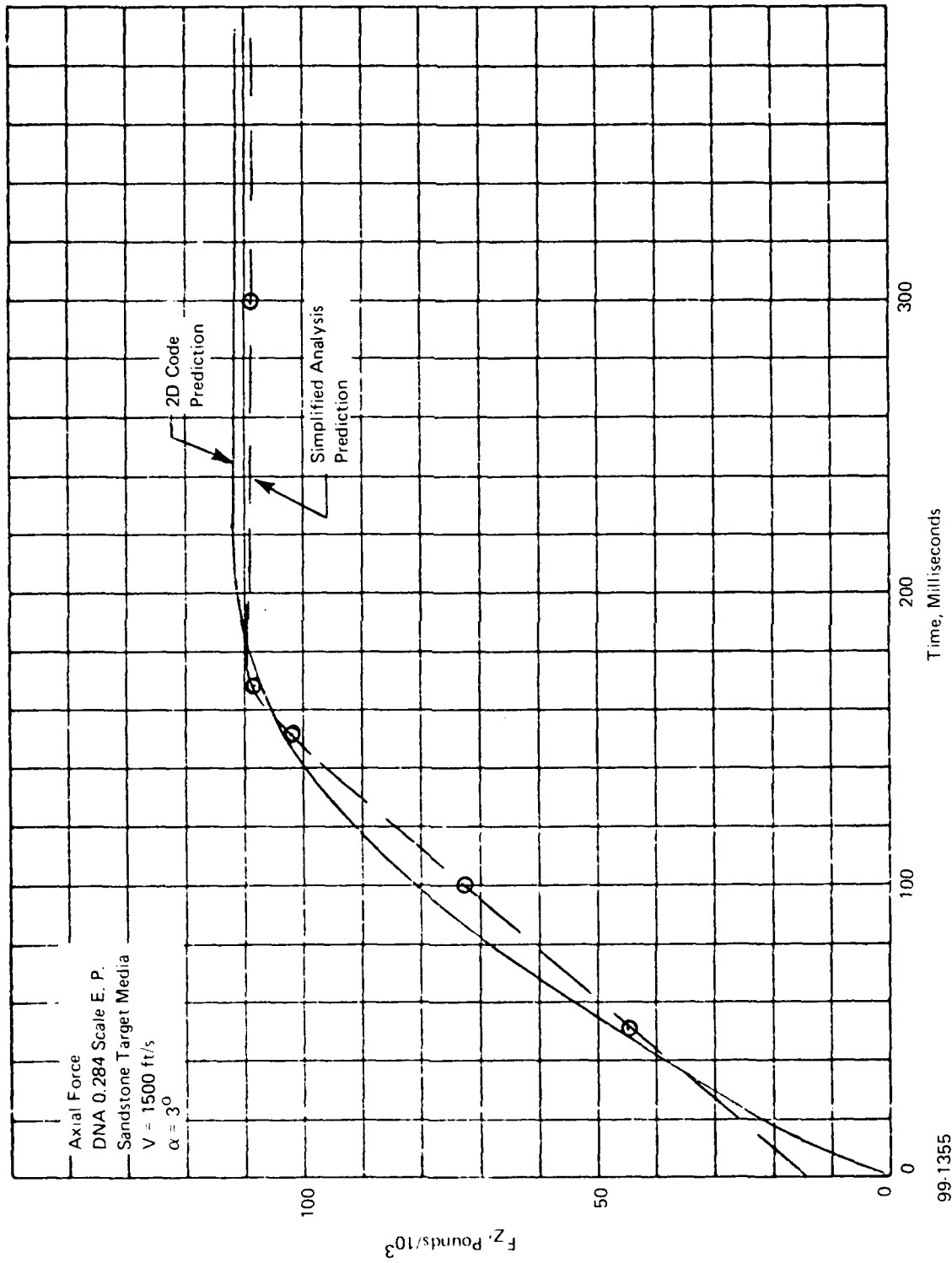


Figure 15 Axial loading comparison — DNA 0.284 scale earth penetrator

99.1355

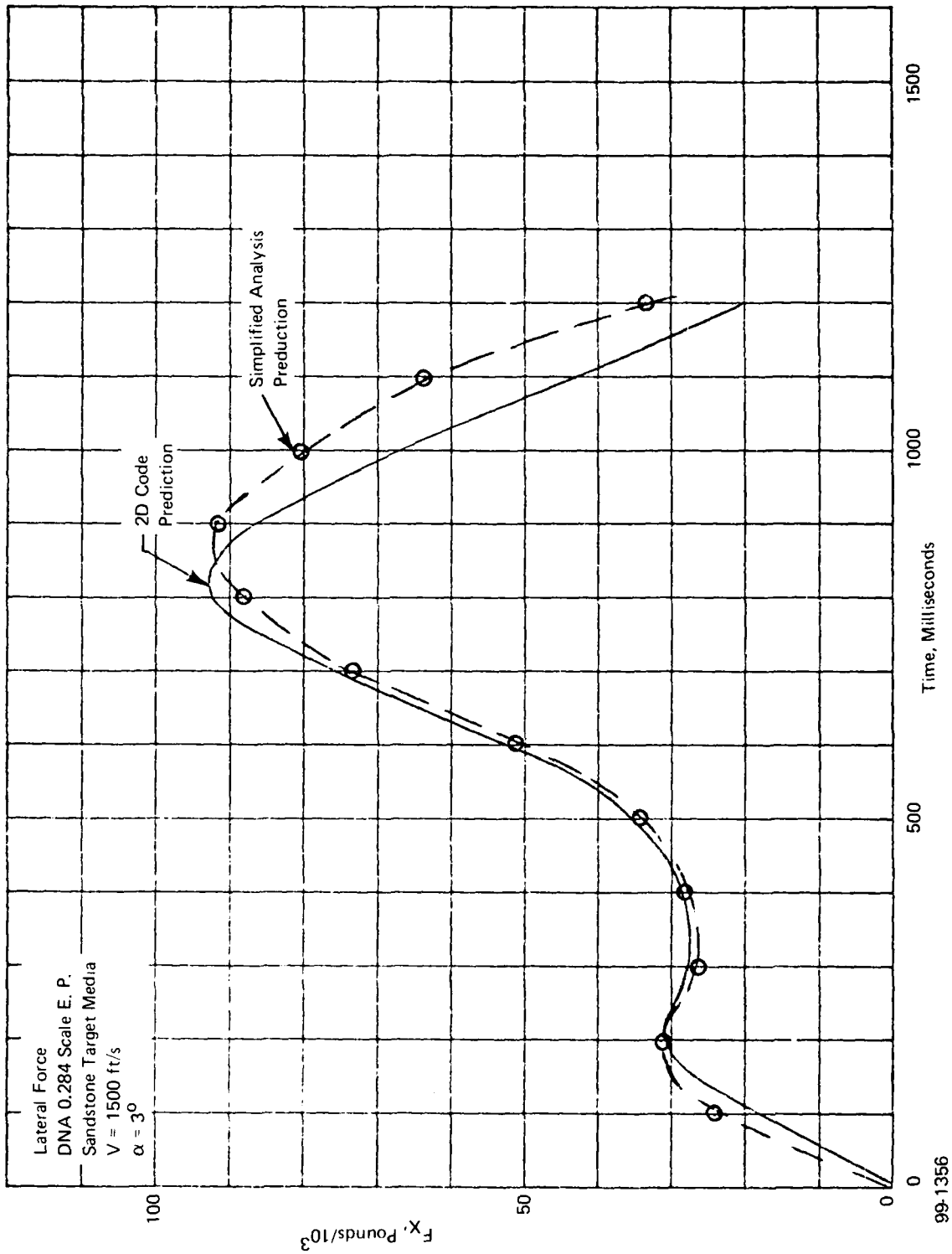


Figure 16 Lateral loading comparison — DNA 0.284 scale earth penetrator

99-1356

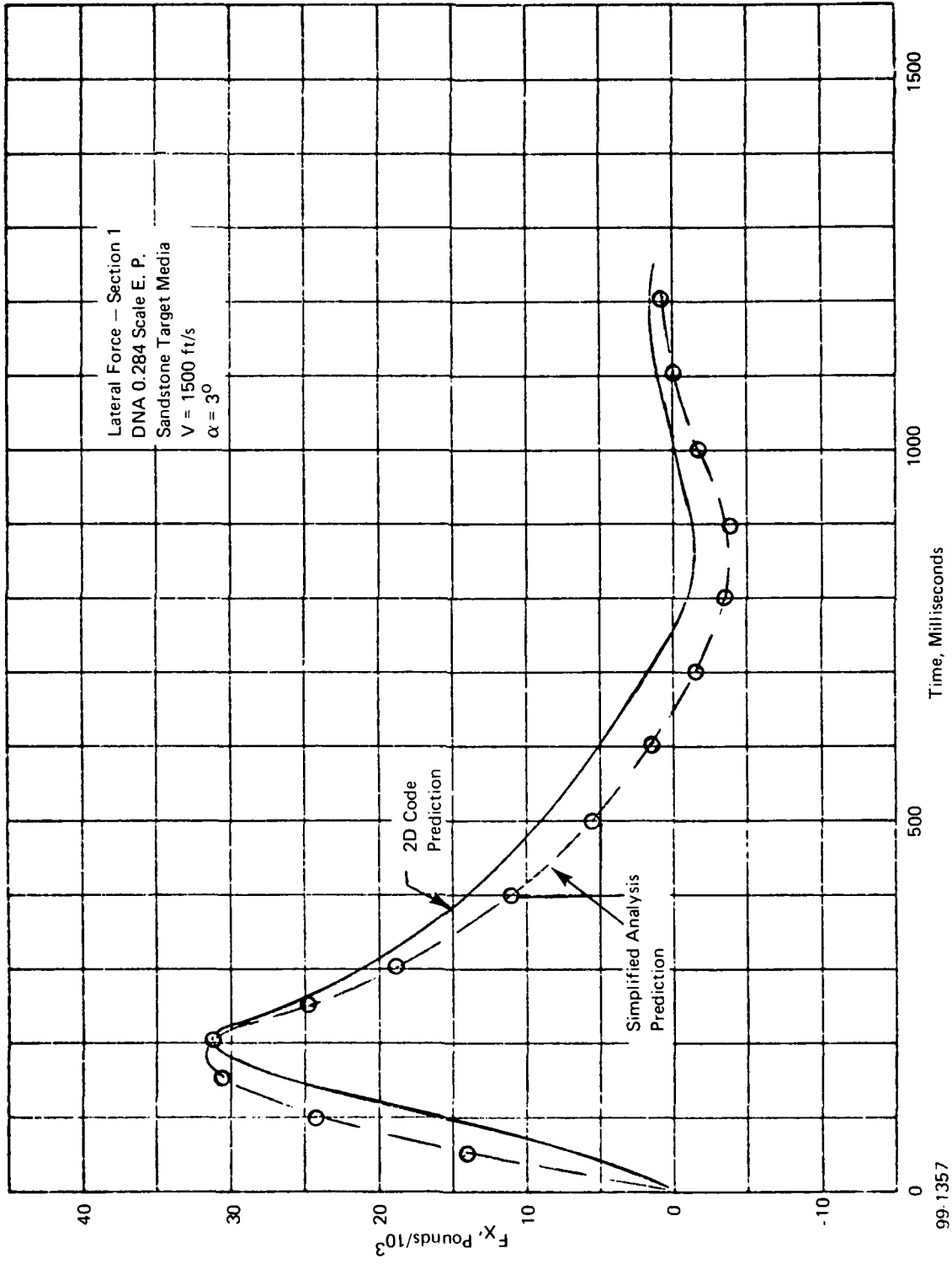


Figure 17 Lateral loading comparison -- DNA 0.284 scale earth penetrator -- Section 1

99-1357

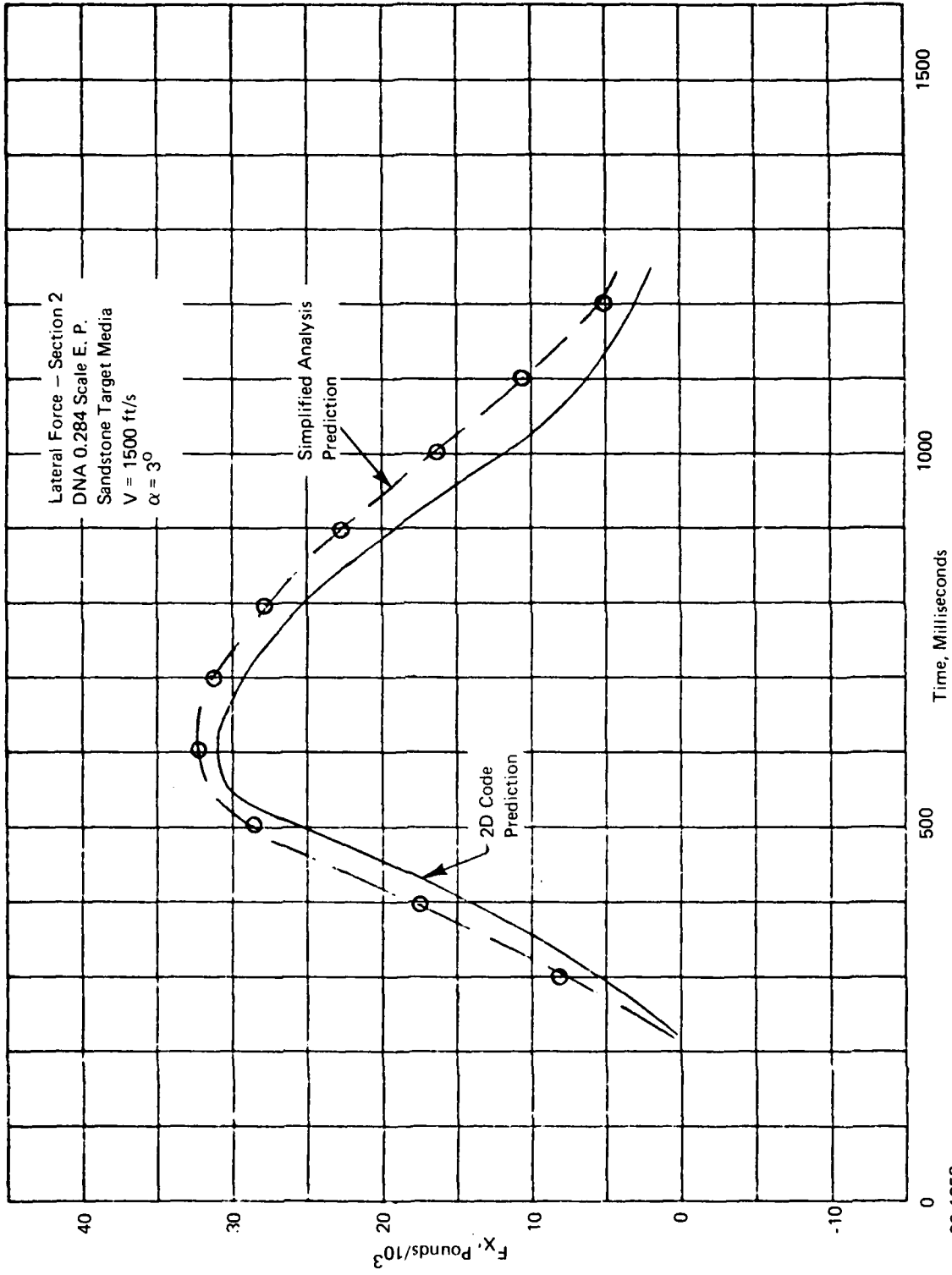


Figure 18 Lateral loading comparison — DNA 0.284 scale earth penetrator — Section 2

99.1358

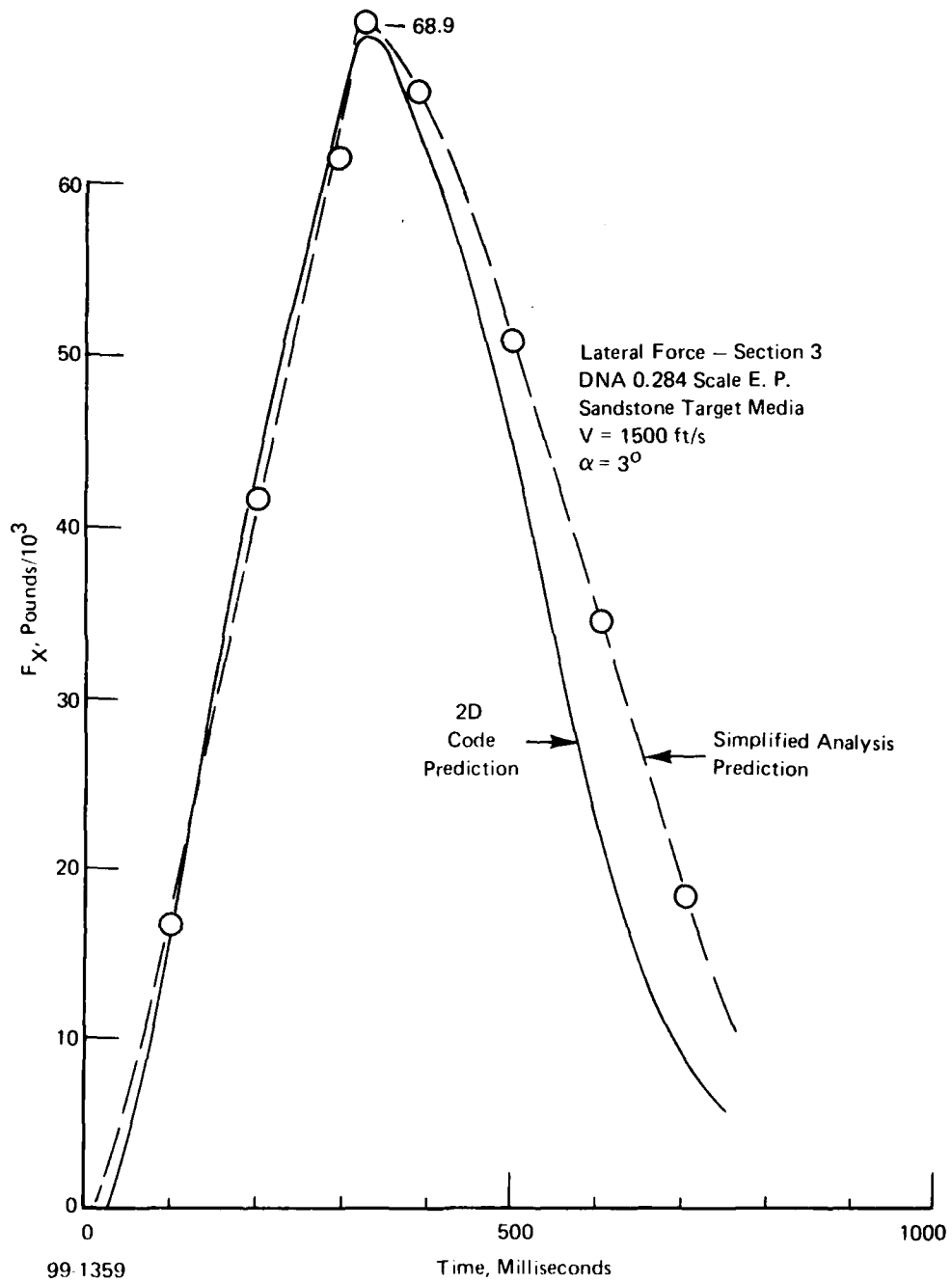


Figure 19 Lateral loading comparison – DNA 0.284 scale earth penetrator – Section 3

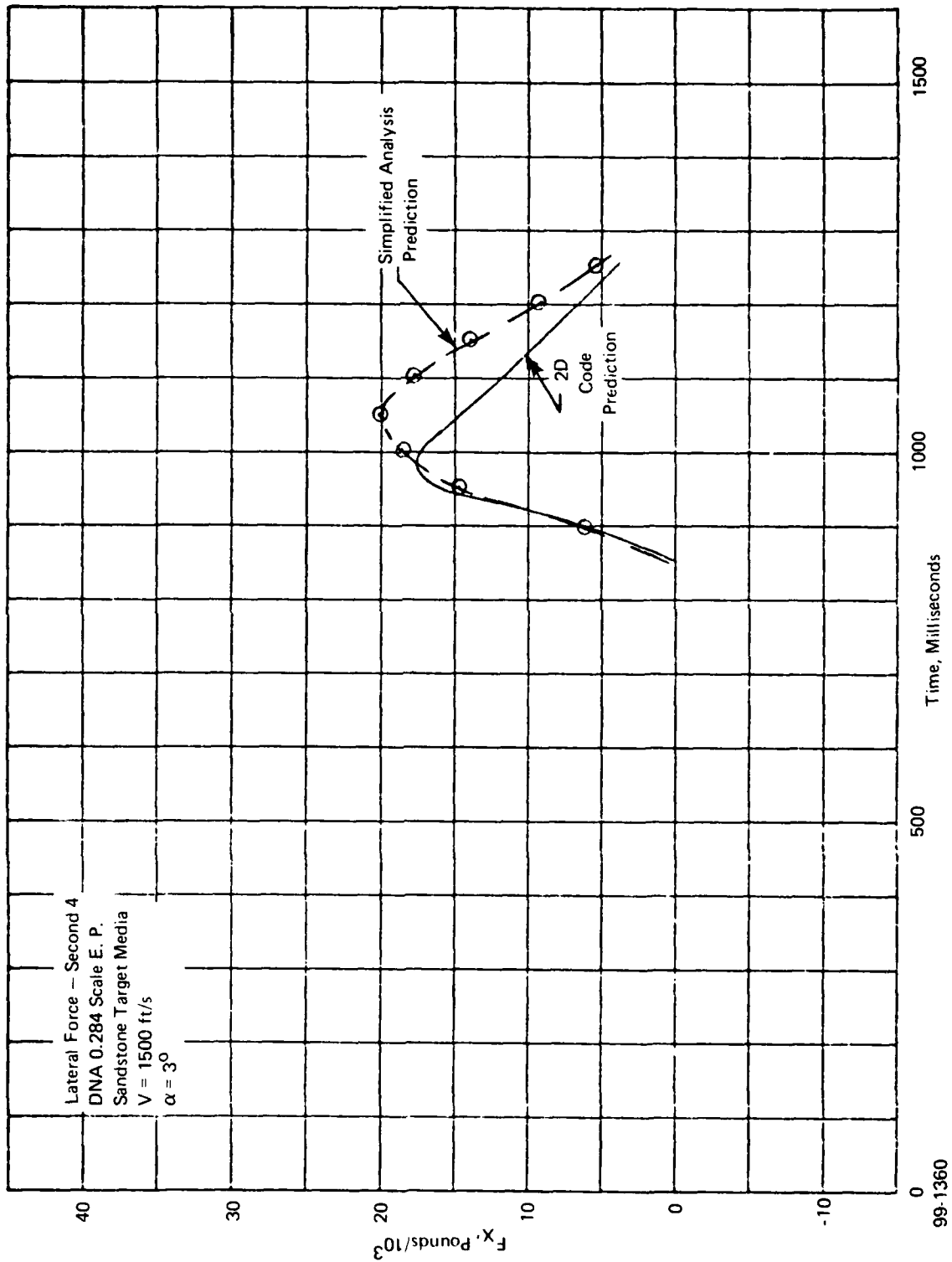


Figure 20 Lateral loading comparison - DNA 0.284 scale earth penetrator - Section 4

99-1360

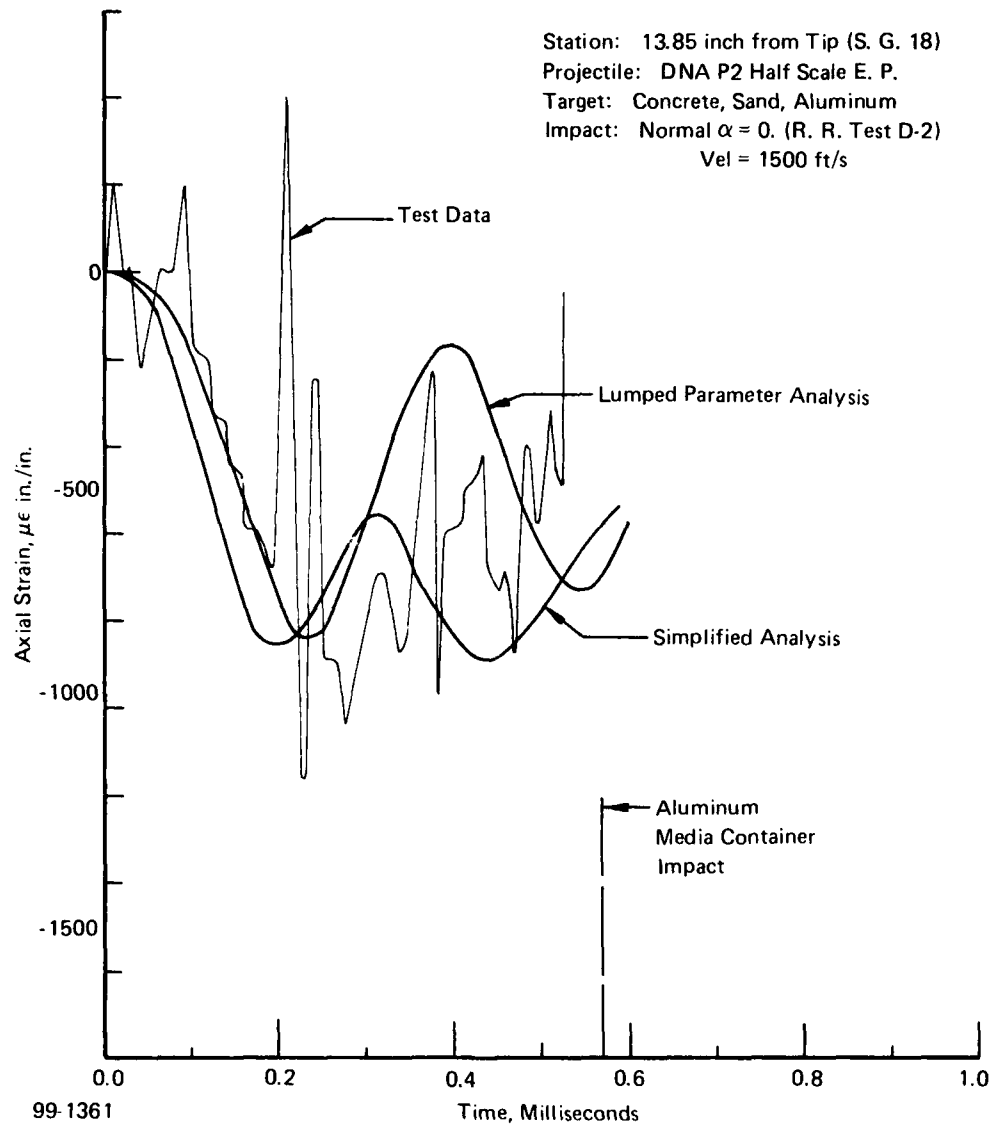
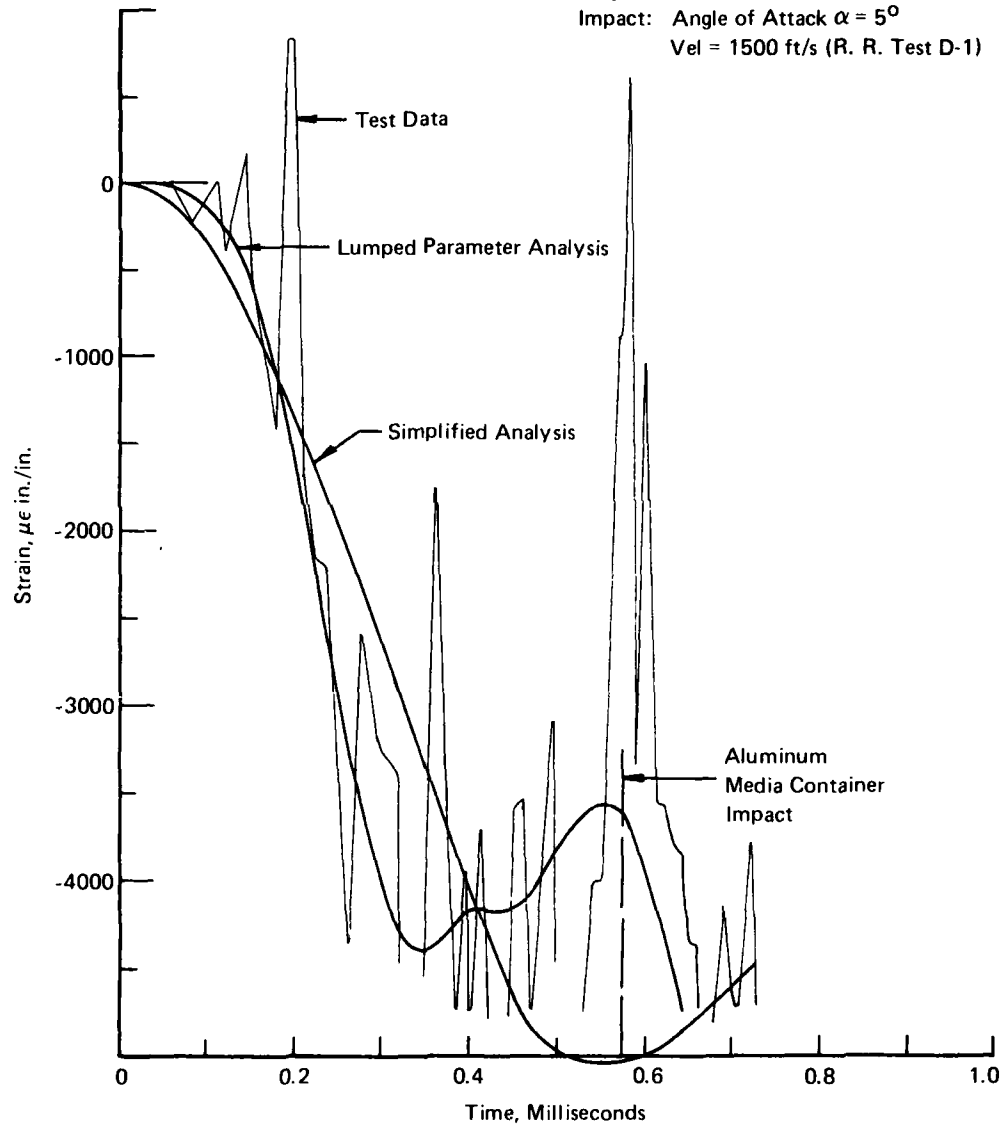


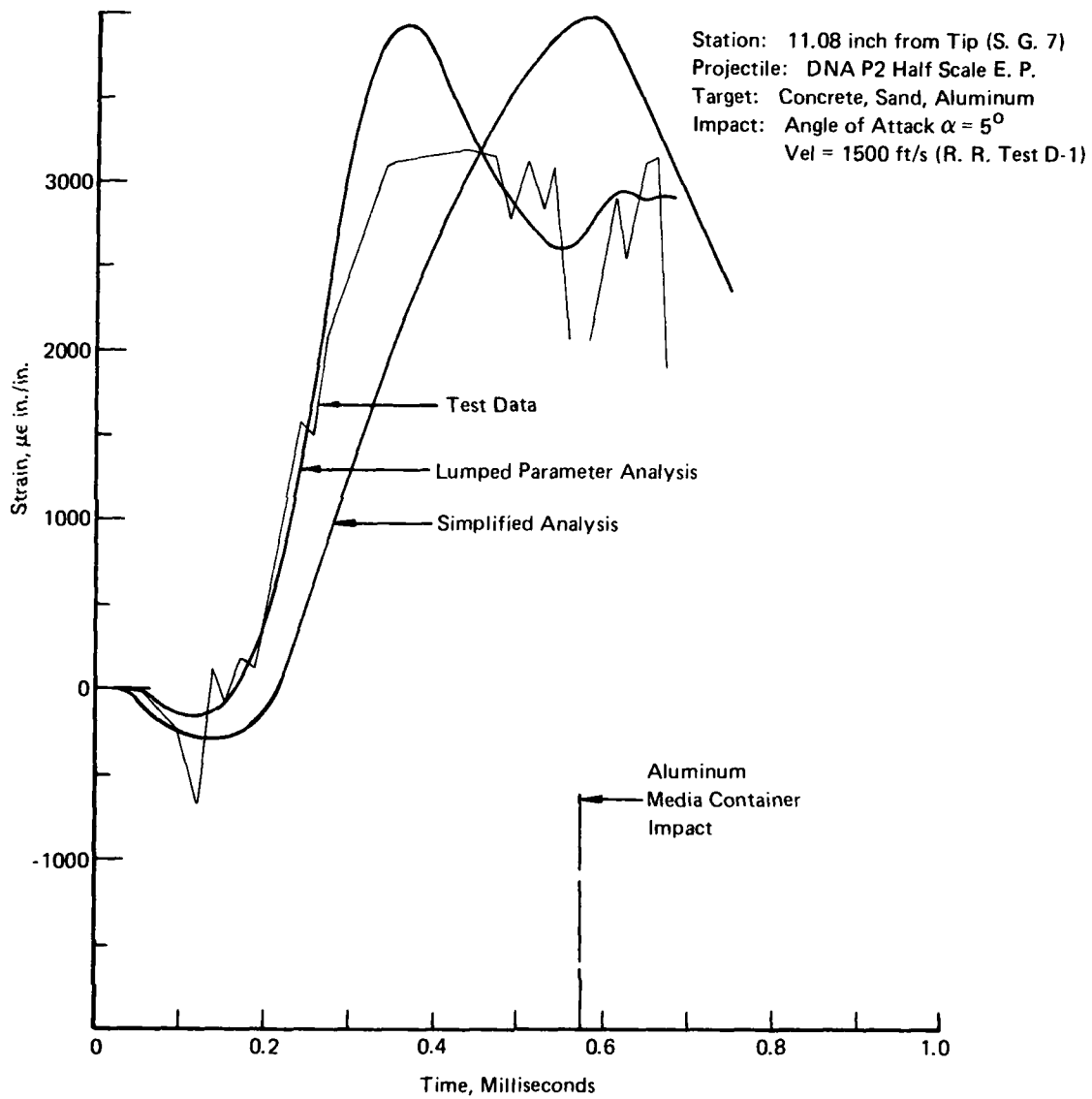
Figure 21 Test data/analysis comparison -- P-2 Half scale earth penetrator -- $\alpha = 0^\circ$

Station: 11.08 inch from Tip (S.G. 5)
Projectile: DNA P2 Half Scale E. P.
Target: Concrete, Sand, Aluminum
Impact: Angle of Attack $\alpha = 5^\circ$
Vel = 1500 ft/s (R. R. Test D-1)



99-1362

Figure 22 Test data/analysis comparison - P-2 Half scale earth penetrator - $\alpha = 5^\circ$



99-1363

Figure 23 Test data/analysis comparison - P-2 Half scale earth penetrator - $\alpha = 5^\circ$

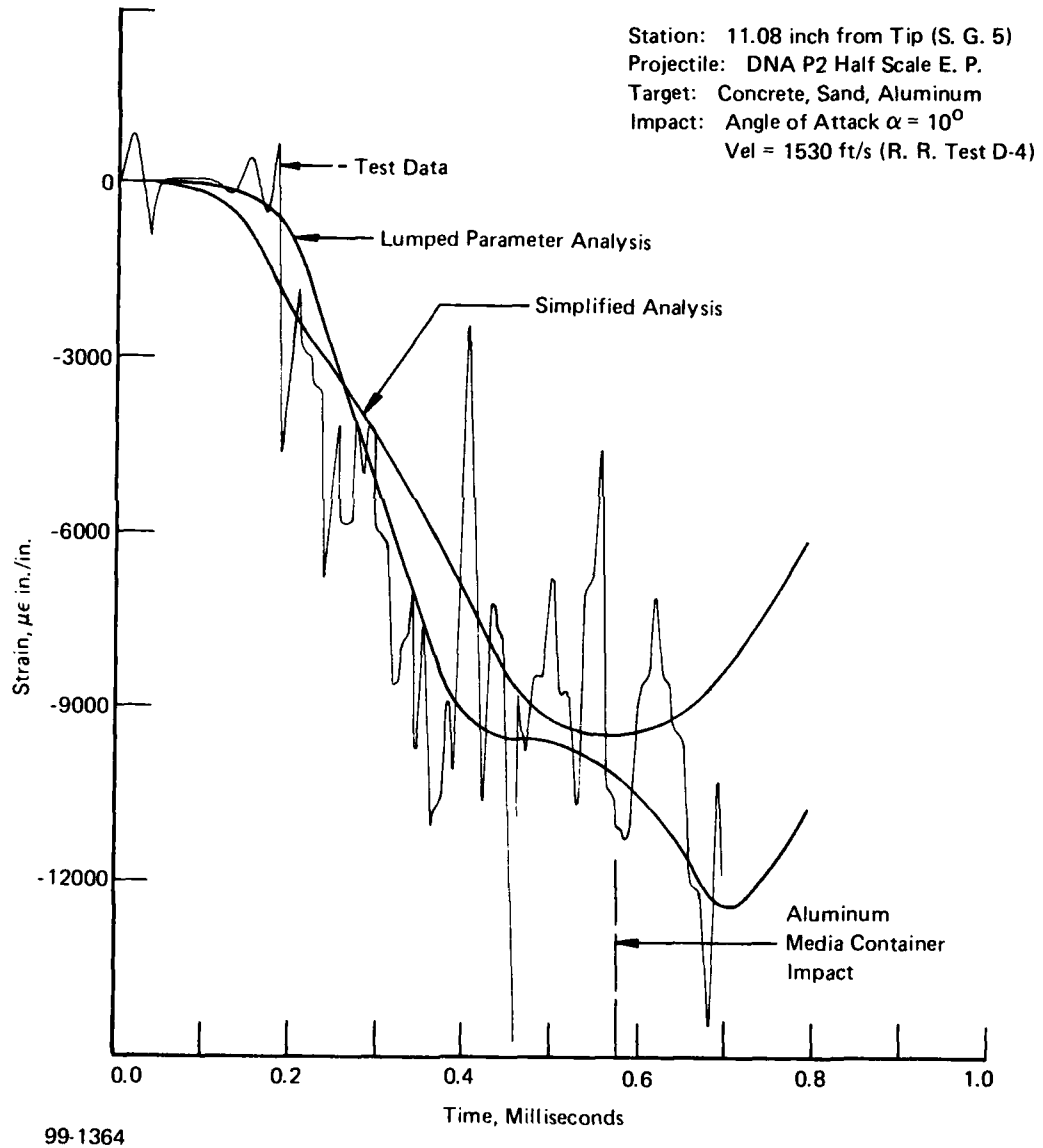
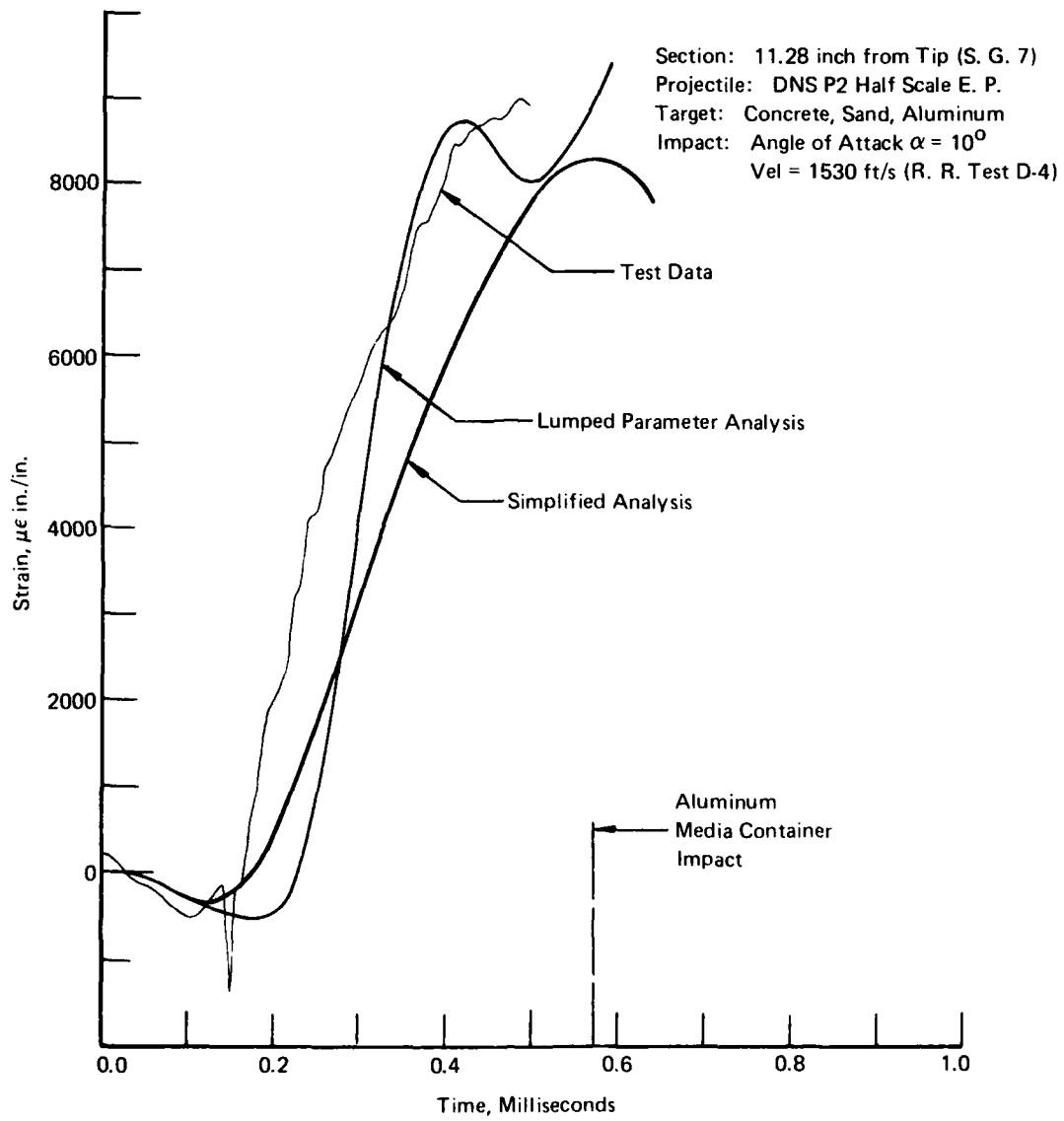


Figure 24 Test data/analysis comparison - P-2 Half scale earth penetrator - $\alpha = 10^\circ$



99-1365

Figure 25 Test data/analysis comparison - P-2 Half scale earth penetrator - $\alpha = 10^\circ$

S. G. 6
DNA 0.284 Scale E. P.
Sandstone Target
V = 1500 ft/s
 $\alpha = 0^\circ$

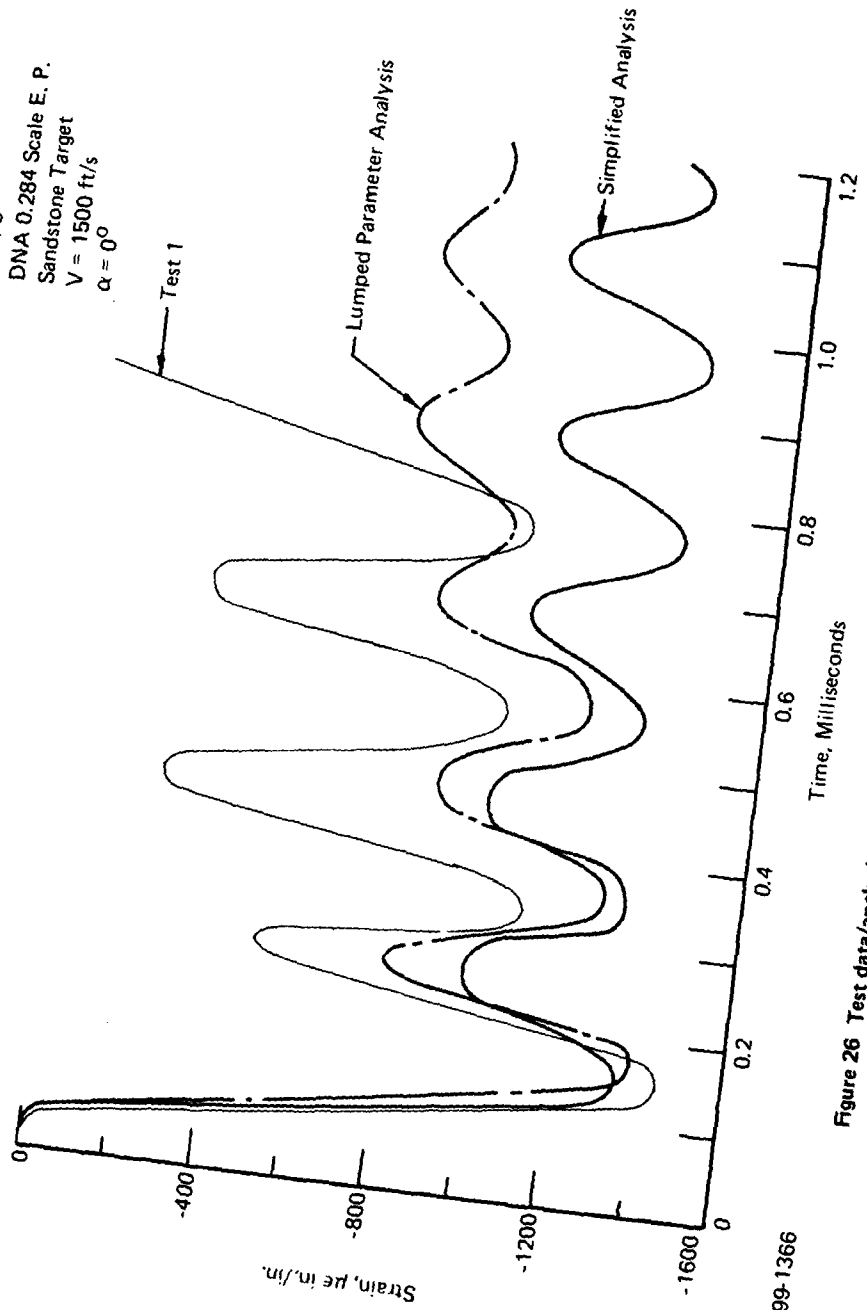
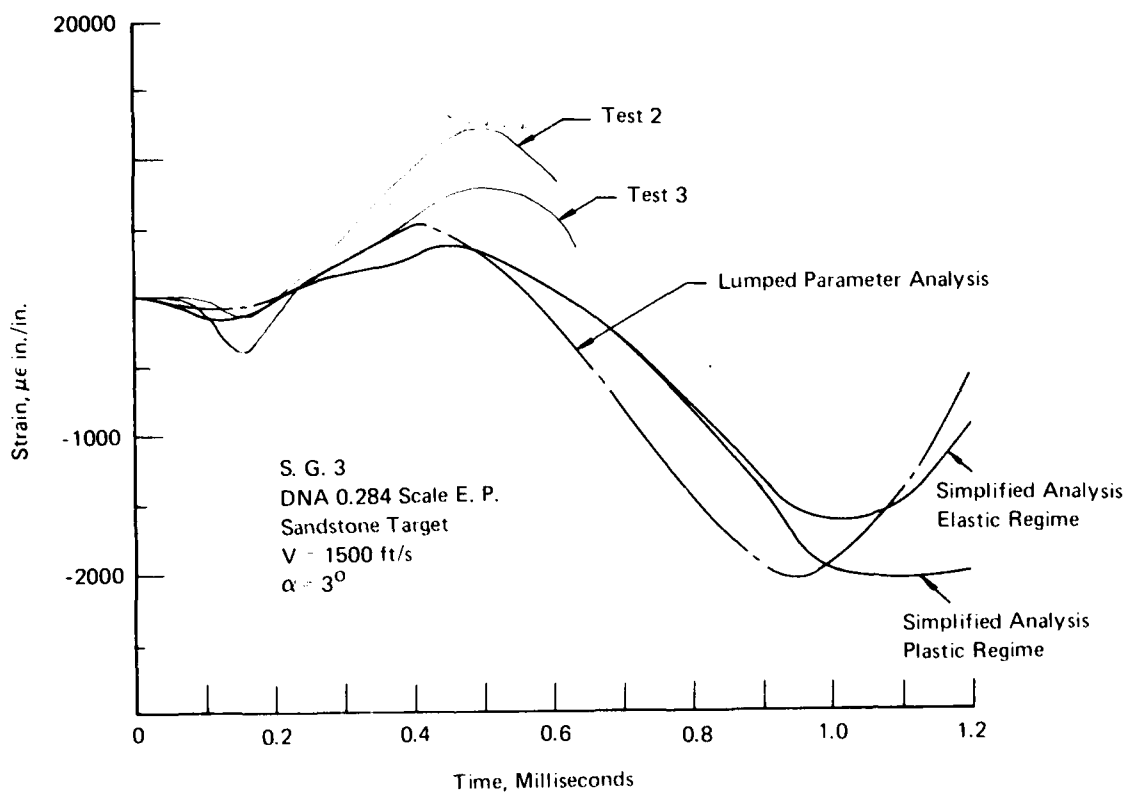
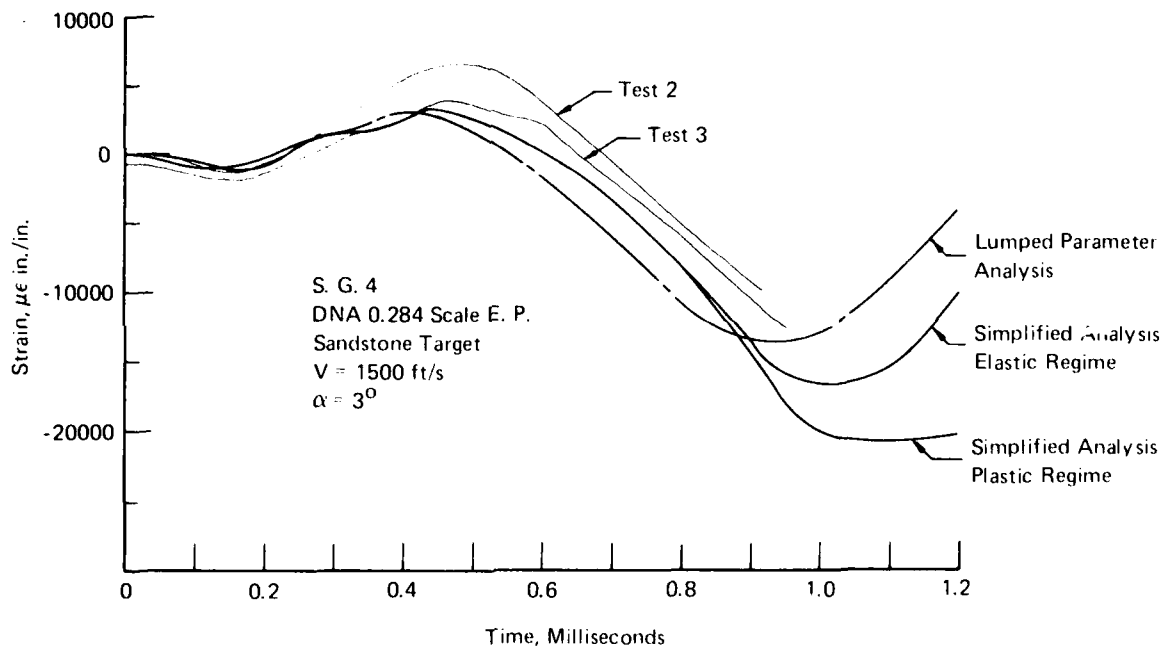


Figure 26 Test data/analysis comparison - DNA 0.284 scale earth penetrator - S.G. 6



99-1367

Figure 27 Test data/analysis comparison – DNA 0.284 scale earth penetrator – S.G. 3



99-1368

Figure 28 Test data/analysis comparison – DNA 0.284 scale earth penetrator – S.G. 4

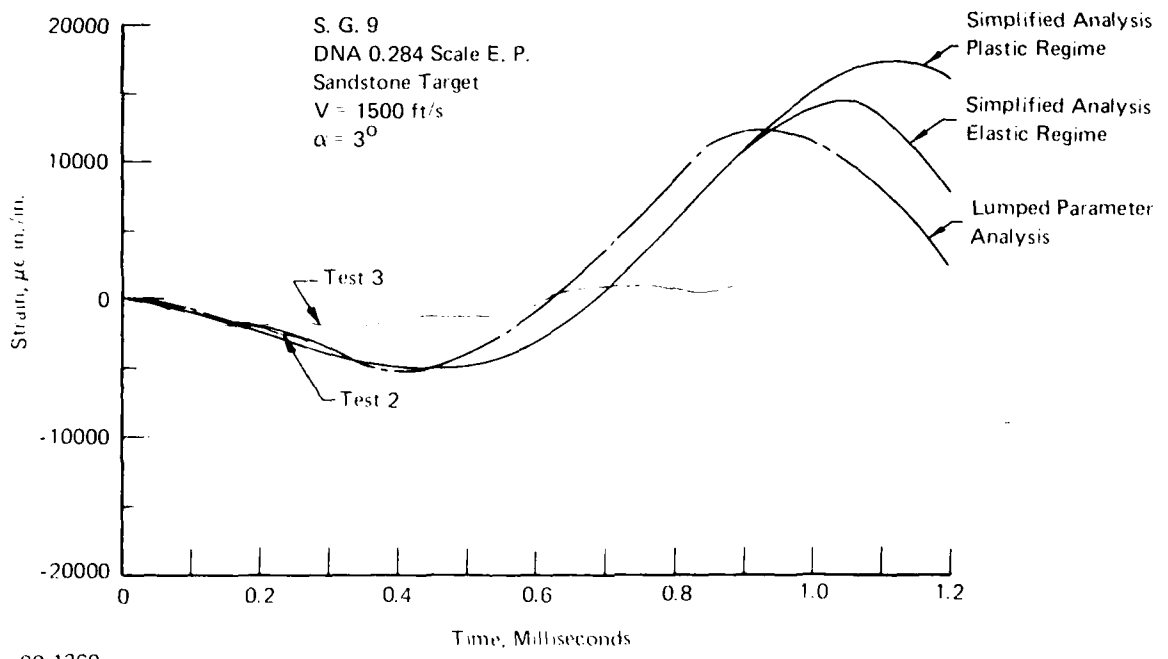
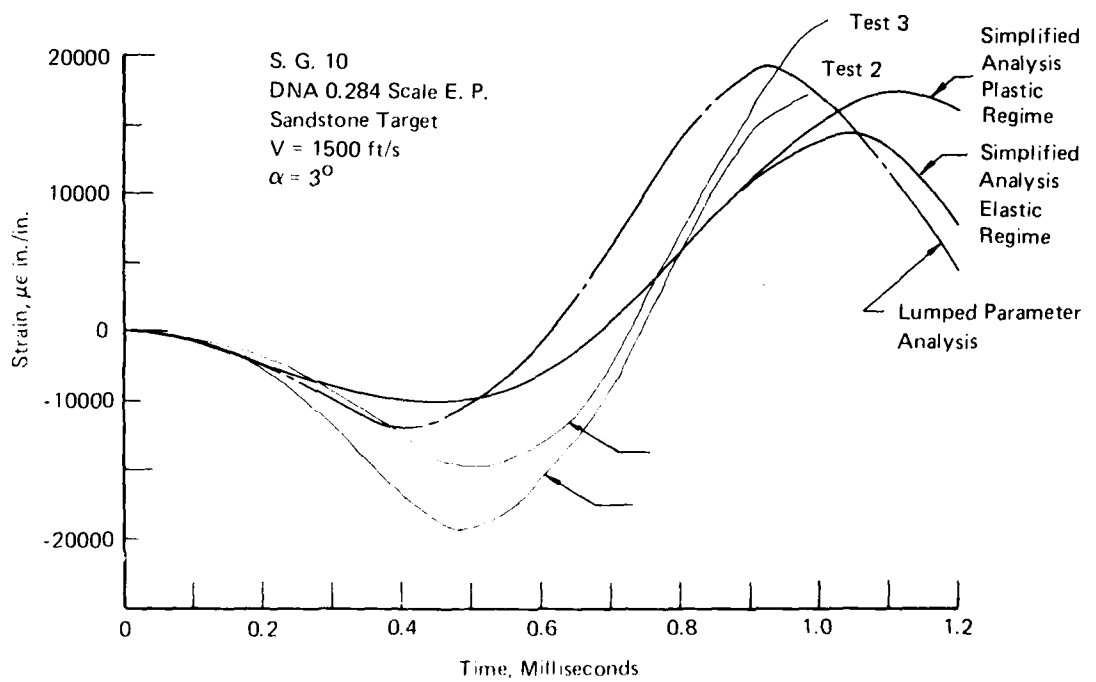


Figure 29 Test data/analysis comparison – DNA 0.284 scale earth penetrator – S.G. 9



99-1370

Figure 30 Test data/analysis comparison -- DNA 0.284 scale earth penetrator -- S.G. 10

SECTION 6.0

PARAMETRIC STUDIES

A series of parametric studies can be performed now that the validity of this simplified structural analysis technique has been verified. The parametric studies encompassed several design factors including impact conditions, material strength, penetrator structural stiffness and penetrator L/D.

The design used in this study is similar to the full scale P-2 earth penetrator, with the flare omitted. The three parameters that were varied in the earth penetrator design studies are:

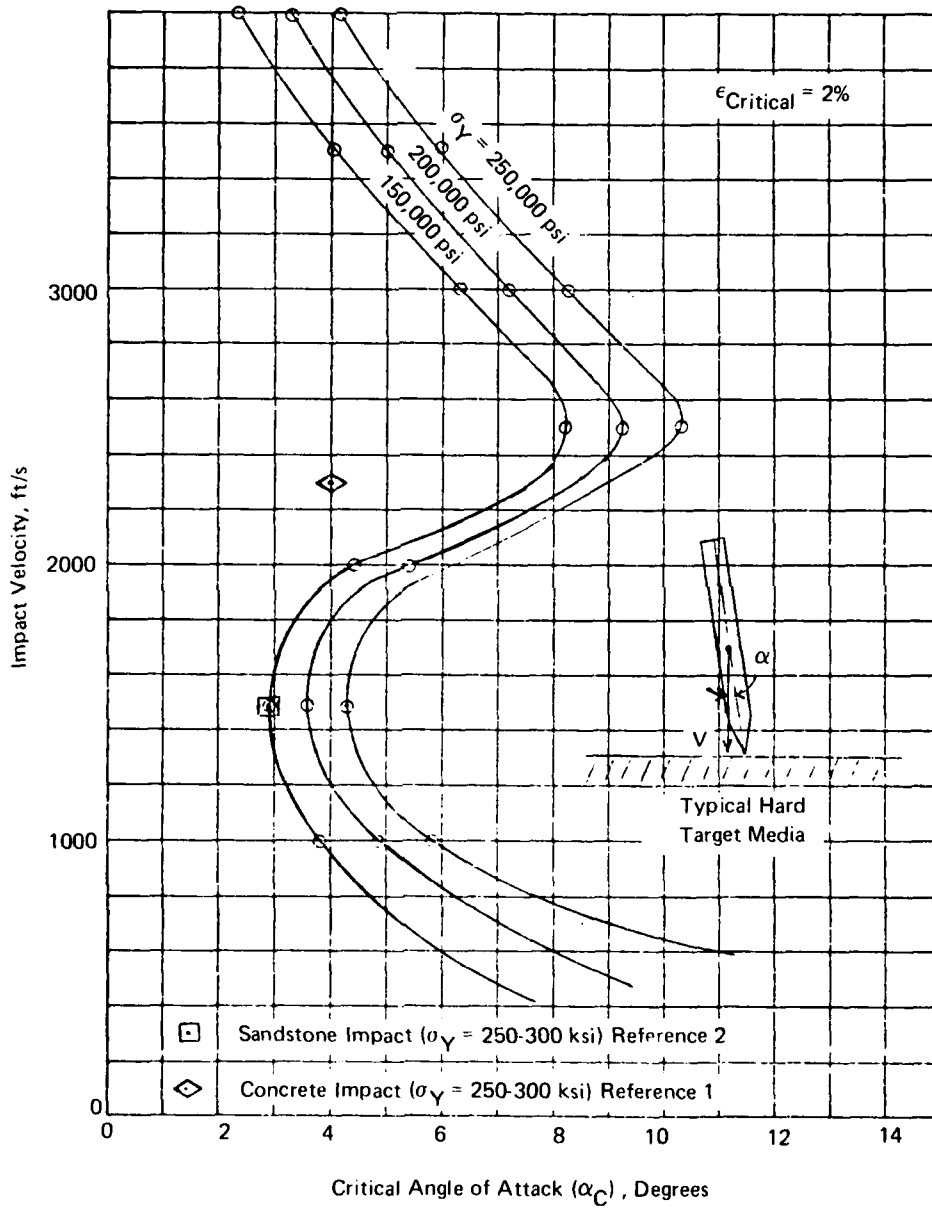
- Material strength.
- Structural ruggedness (i.e., wall thickness).
- Length to diameter ration (L/D).

All analyses consisted of varying impact conditions. The range of the impact conditions were:

- Sandstone target media.
- Normal target media obliquity.
- Impact velocity from 1000 to 4000 ft/s.
- Angle of attack from 0 to 15 degrees.

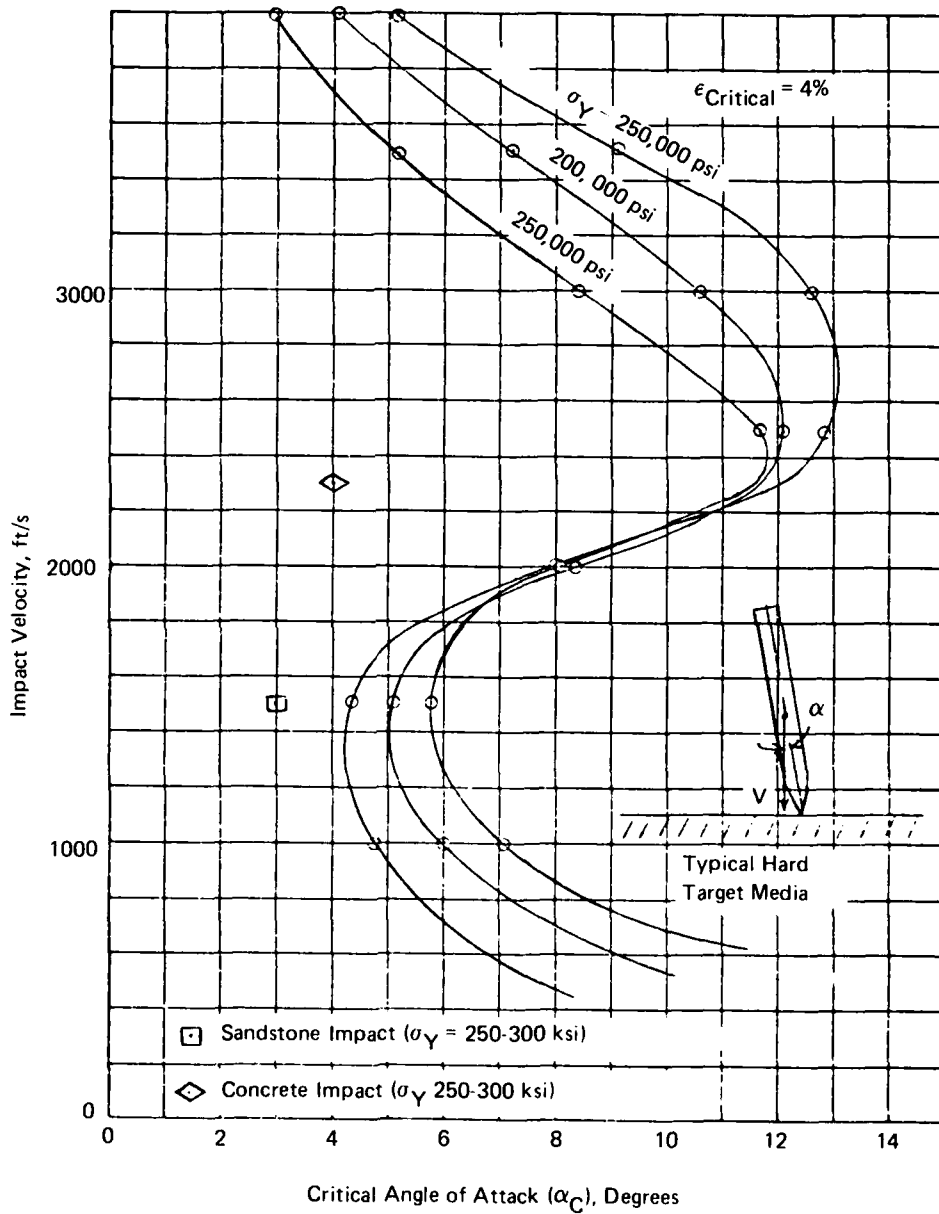
The sandstone target media was chosen as representative of a hard media (e.g., concrete, rock, etc.), and because penetrator structural survival is design critical for high strength media, the softer target media were not considered. Normal obliquity was imposed by the limitations of the current simplified procedure, although impact obliquities up to 45 degrees should not substantially alter the results. The impact velocity and angle of attack were varied over the ranges specified to determine the limits of structural survivability. The impact velocity range was sampled at 500 ft/s intervals with angle of attack being increased until the design failure criteria of structural survivability was exceeded. In general this criteria was a function of allowable plastic deformation. The incrementing of the velocity and angle of attack was handled automatically by the code.

The first parametric study considered the effect of penetrator material strength on capability. Three yield strengths were selected, 150, 200, and 250 ksi. The results are shown on Figures 31, 32 and 33 for strain allowables of 2, 4, and 6 percent, respectively. The presentation format of the results show impact velocity versus critical (maximum) angle of attack which will produce the allowable strain. Also included are two test data points for



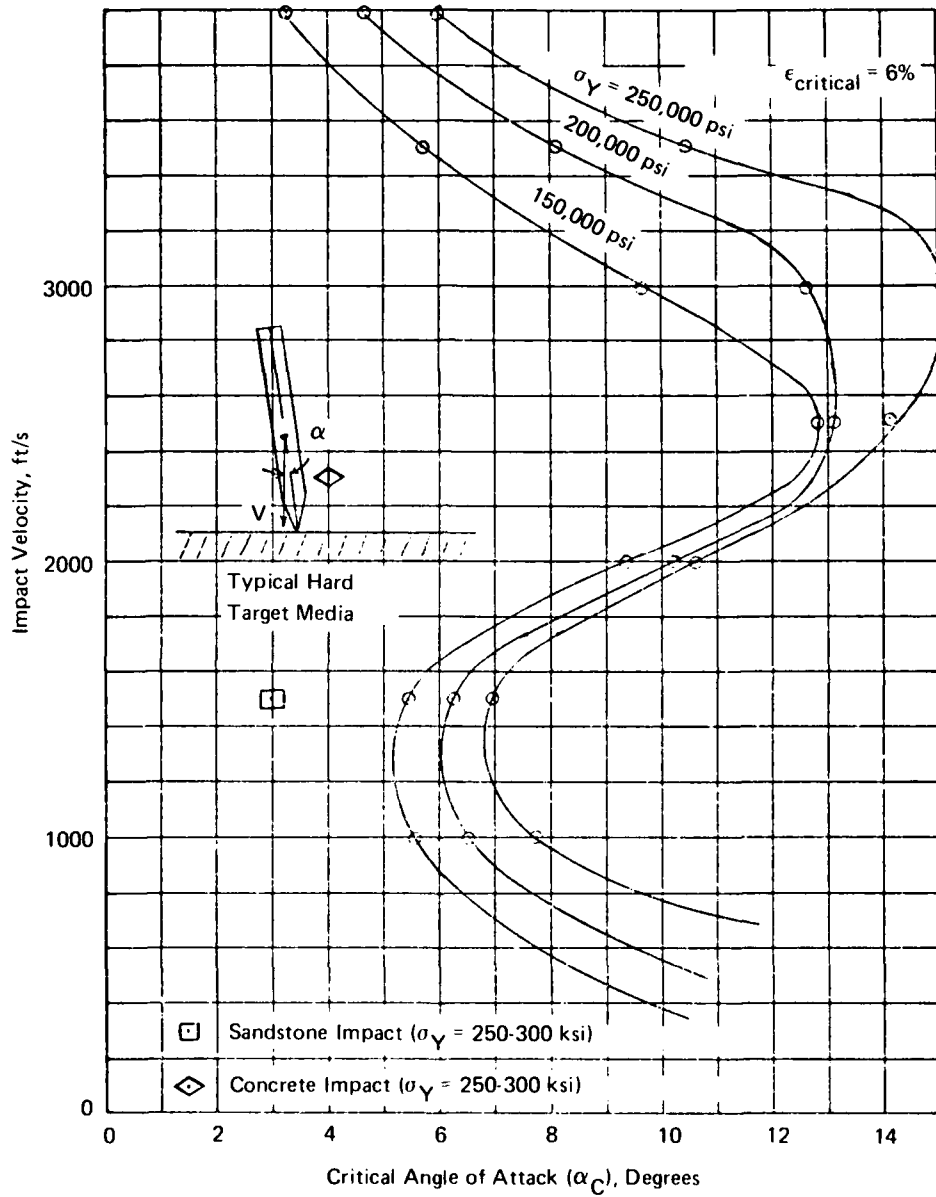
99-1371

Figure 31 Parametric study results — structural material — $\epsilon_{\text{critical}} = 2\%$



99-1372

Figure 32 Parametric study results — structural material — $\epsilon_{\text{critical}} = 4\%$



99-1373

Figure 33 Parametric study results — structural material — $\epsilon_{\text{critical}} = 6\%$

correlation, one from the reverse ballistic sled tests (Reference 2) at $\alpha = 3$ degrees and the other from concrete reverse ballistic impact tests (Reference 1).

These figures show some surprising trends. The most important of which is the sharp inflection of the curves in the velocity regime of 2000 to 3000 ft/s. Instead of following the expected behavior exhibited in the 0 to 1500 ft/s, i.e., as velocity is increased the critical angle of attack at which failure is predicted decreases, the results indicate that structural survivability can improve with higher impact velocities (1500 to 2500 ft/s). Also the results show that very high velocities (i.e., >3000 ft/s) are required to produce the same critical angle of attack for failure as expected at 1500 ft/s.

A detailed review of the equations of motion that produce these results was performed to verify the procedure. A graphic explanation of this phenomena is provided on Figure 34. The figure shows an impact event, with and without the effect of rigid body motion included. The impact for the left hand portion of the figure (without rigid body motion) is described below. At time $t(1)$ the E.P. first impacts the target media. At time $t(2)$ nose wetting is achieved and the lateral surface loading produces a bending moment distribution in the expected direction (i.e., compression on the upper surface and compression on the lower surface) along the length of the penetrator. This is shown in the strain response shown on the lower left corner of Figure 34. The response of the penetrator with an increase in velocity would show with this analytical model an increase in the lateral loads and bending moments and therefore lower critical angles of attack.

If the effect of rigid body motion is included in the analysis, the penetrator impact history and loads are shown in the right hand column of Figure 34. The impact event is identical with or without the effect of rigid body motion up to time $t(2)$. And until now this has been the result that was predicted. But, now at time $t(3)$ with the rigid body motion included, a pitching motion develops which causes the nose loading to reverse direction. Also, at the same time, lateral loads are being applied to the midsection of the penetrator. It is the combination of both of these loadings that causes a reversal in the bending response of the penetrator. Thus the rate of loading reversal, which is a function of the velocity of the penetrator, can cause a resonance condition, if it is similar to the fundamental frequency of the penetrator. Thus, there is a definite relationship between the impact velocity (which determines how fast the penetrator is loaded or wetted) and the structural response frequency of the penetrator. Velocities which load the penetrator body before penetrator fundamental response frequencies begin are preferred to the lower velocities which cause resonance induced amplification of the fundamental bending mode strains.

To demonstrate this phenomena the distributed loads from the detailed 2-D codes are presented. The example case is a 3 degree angle of attack impact (Reference 2) and the distributed loads at 200, 500 and 800 usecs are presented. An inspection of the first column on Figures 35 through 37, which is the lateral loading distribution (FXPSV), does show the nose load reversal at the same time as peak midsection loads occur.

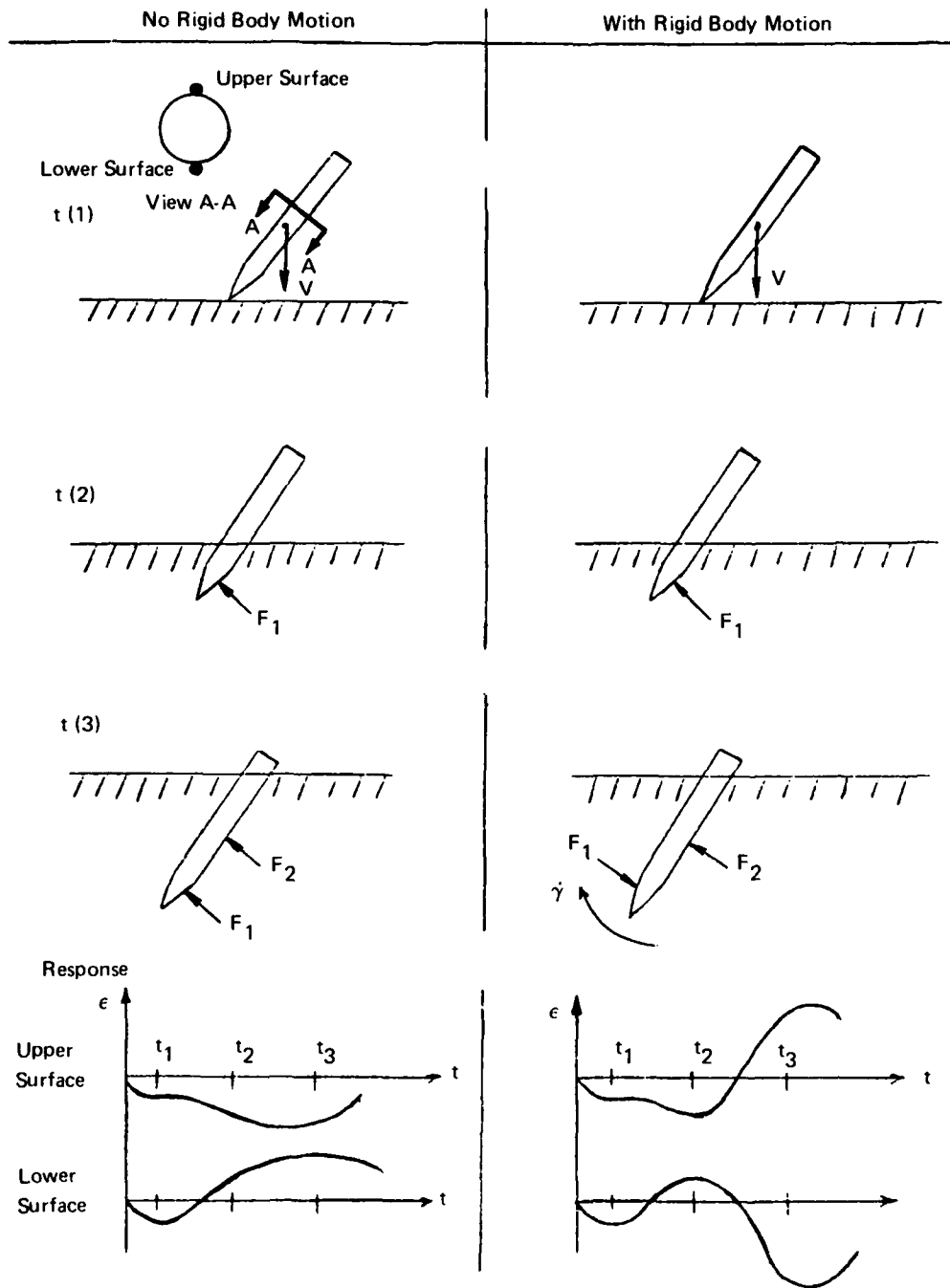


Figure 34 Significance of rigid body motion on loads and response

This confirms the loading reversal which was seen on Figures 31 through 35, and causes an inflection in the capability at velocities above 1500 ft/s. The second reversal at velocities above 2500 ft/s indicates that the overall loading environment is much too severe for the described mechanisms to ensure structural survival.

Another interesting result of the parametric study (Figures 31 through 33), is the effect of reducing the penetrator material allowable from 250 to a 150 ksi (a reduction of 40%). The capability analyses indicate only a 20 to 30 percent reduction in critical angle of attack, which may provide a rationale for performing material allowable strength tradeoff studies to obtain a small reduction in structural survival when cost becomes a major factor in the design.

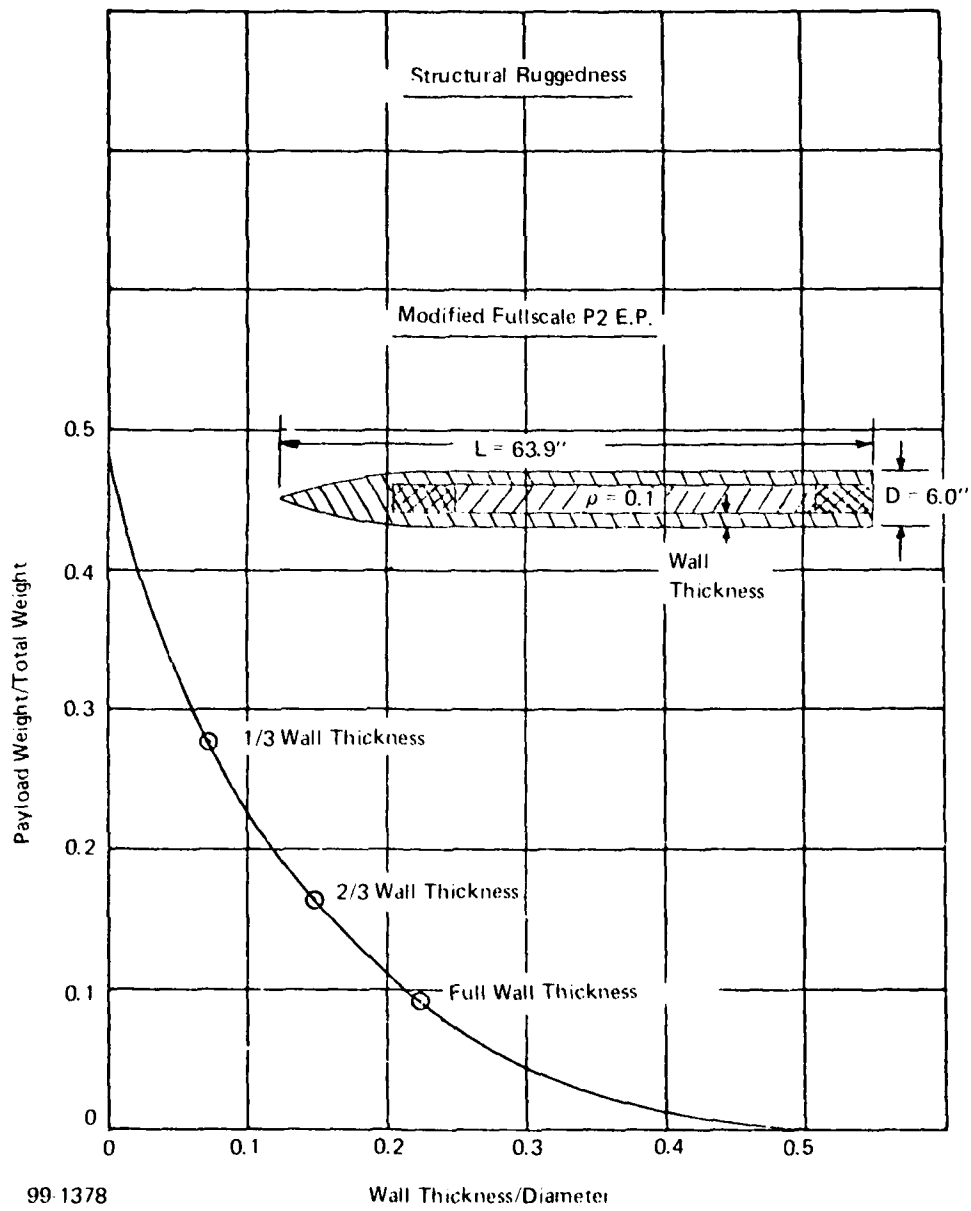
Another result is the 10 to 30 percent increase in critical angle of attack for every 2 percent the critical strain is increased. (See Figures 31 and 32.) The study also indicates that a 150 ksi material with an $\epsilon_{\text{critical}}$ of 4 percent trades-off better than a 250 ksi material with an $\epsilon_{\text{critical}}$ of 2 percent. These results emphasize that tradeoff studies of material strength and elongation properties are significant because design optimization can be realized without sacrificing structural integrity.

The second parametric study considered the effect of penetrator wall thickness on structural survivability. Before performing the parametric study a demonstration of the effect of optimizing the wall thickness will be made. On Figure 38, for the specific penetrator shown ($L = 63.9$ in, $D = 6.0$ in), the effect of reducing the wall thickness and thereby increasing the available volume (a function of payload weight) for payload packaging is shown. This indicates the effect of wall thickness reduction on payload available weight.

The parametric study considered three wall thicknesses expressed in terms of a non-dimensional parameter by dividing by the penetrator diameter t/D 0.225, 0.150, and 0.075. These represent the baseline design thicknesses, two thirds of the baseline design and one third of the baseline design thickness. The baseline configuration is the full scale DNA earth penetrator with a nominal material yield strength of 200 ksi. The study was performed with the following impact parameter ranges: the impact velocity was varied from 1000 to 4000 ft/s and the angle of attack from zero until the structural criteria was exceeded. The results are shown on Figures 39, 40, and 41 for various strain allowable values. As seen in the first parametric study, the figures show the resonance phenomena occurring around 1000 ft/s.

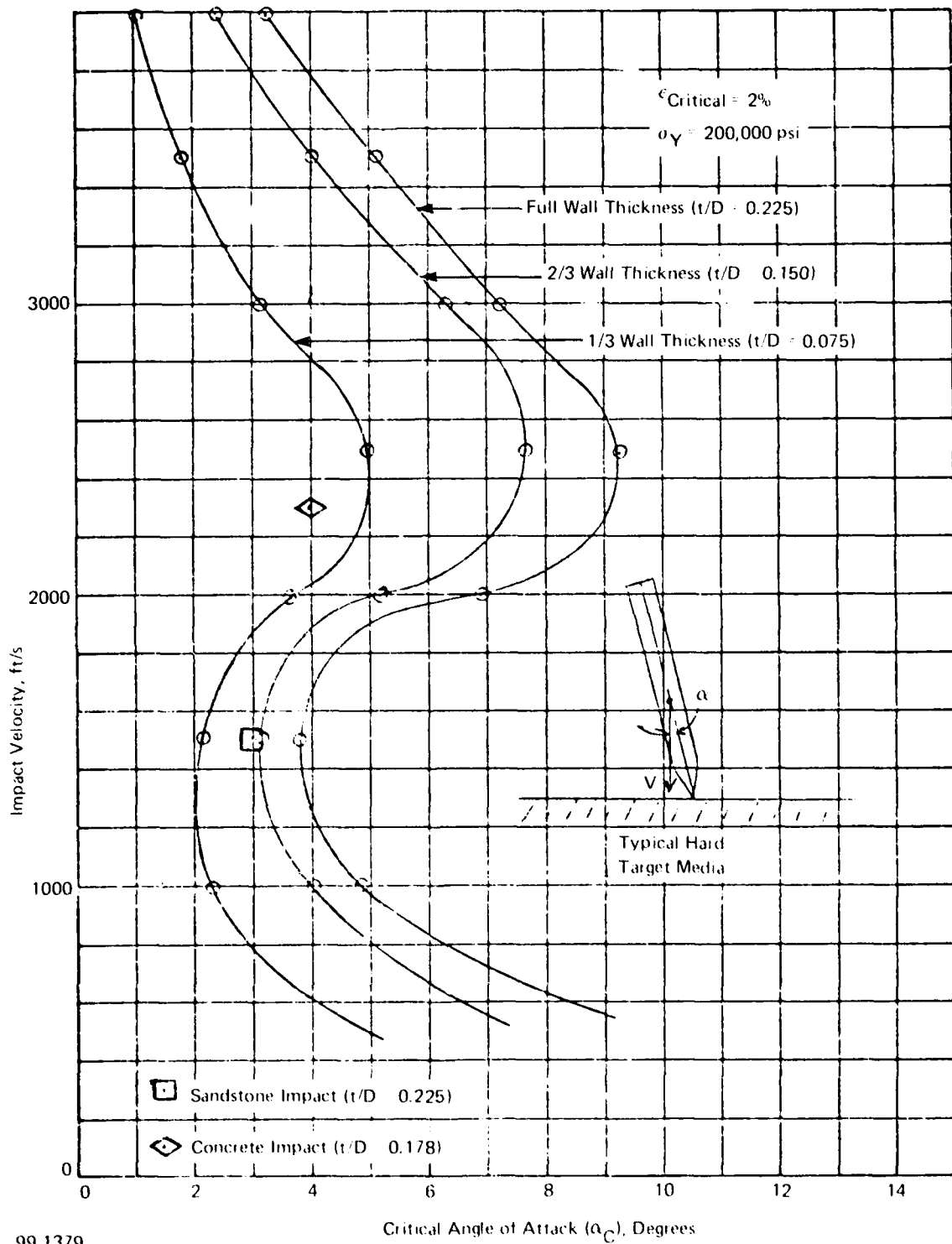
The significant conclusion from this study is that only a relatively small survivability penalty results from a reduction in the wall thickness. A 1/3 reduction in wall thickness (i.e., 2/3 baseline) produces only a 10 to 20 percent reduction in critical angle of attack while a 2/3 reduction in wall thickness (i.e., 1/3 baseline) yields only a 40 to 60 percent reduction in critical angle of attack. These results indicate the importance of tradeoff studies in penetrator design.

The final parametric study involved the effect of variations in penetrator length to diameter ratio (L/D) on survivability. The values of L/D selected



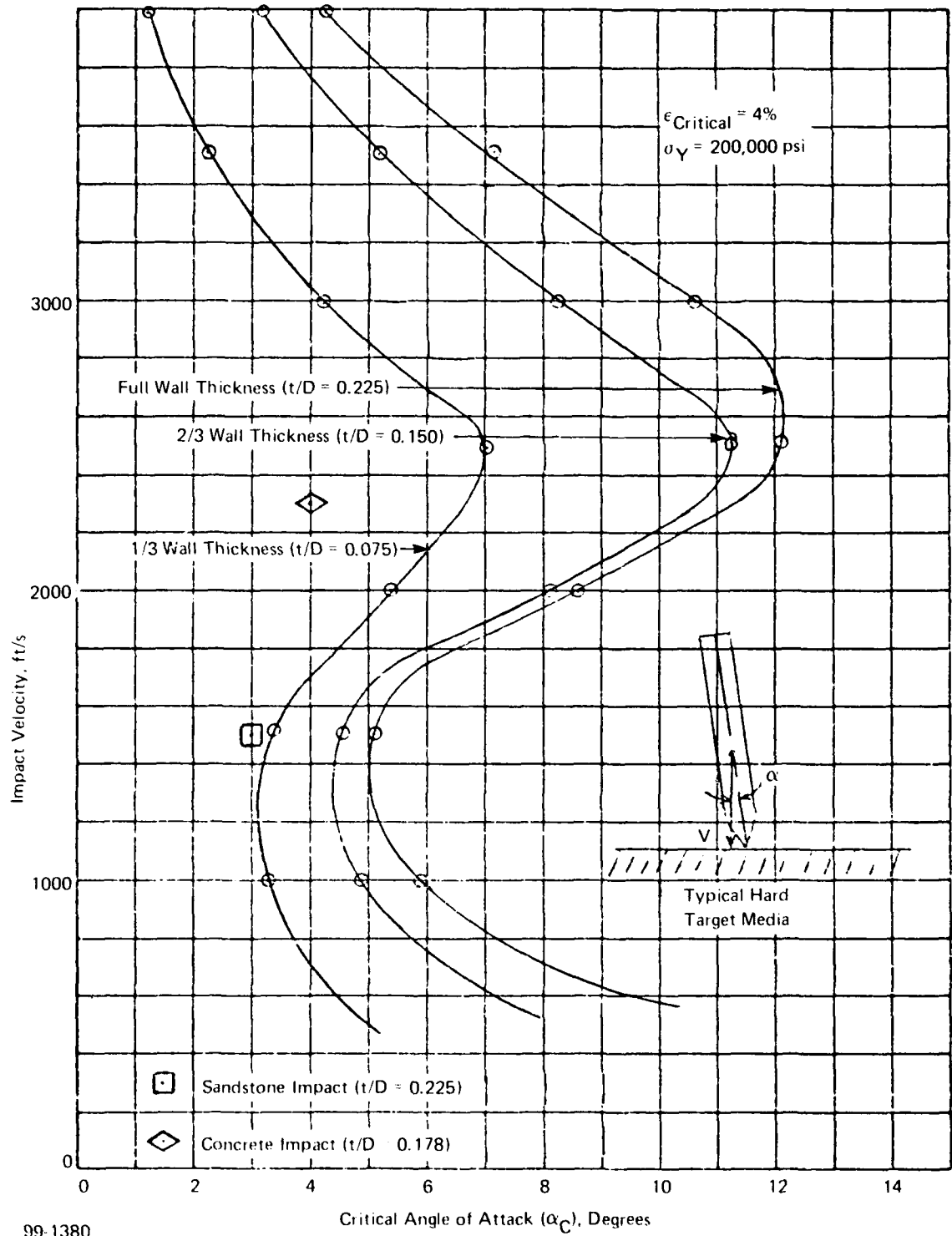
99-1378

Figure 38 Penetrator configurations – structural ruggedness



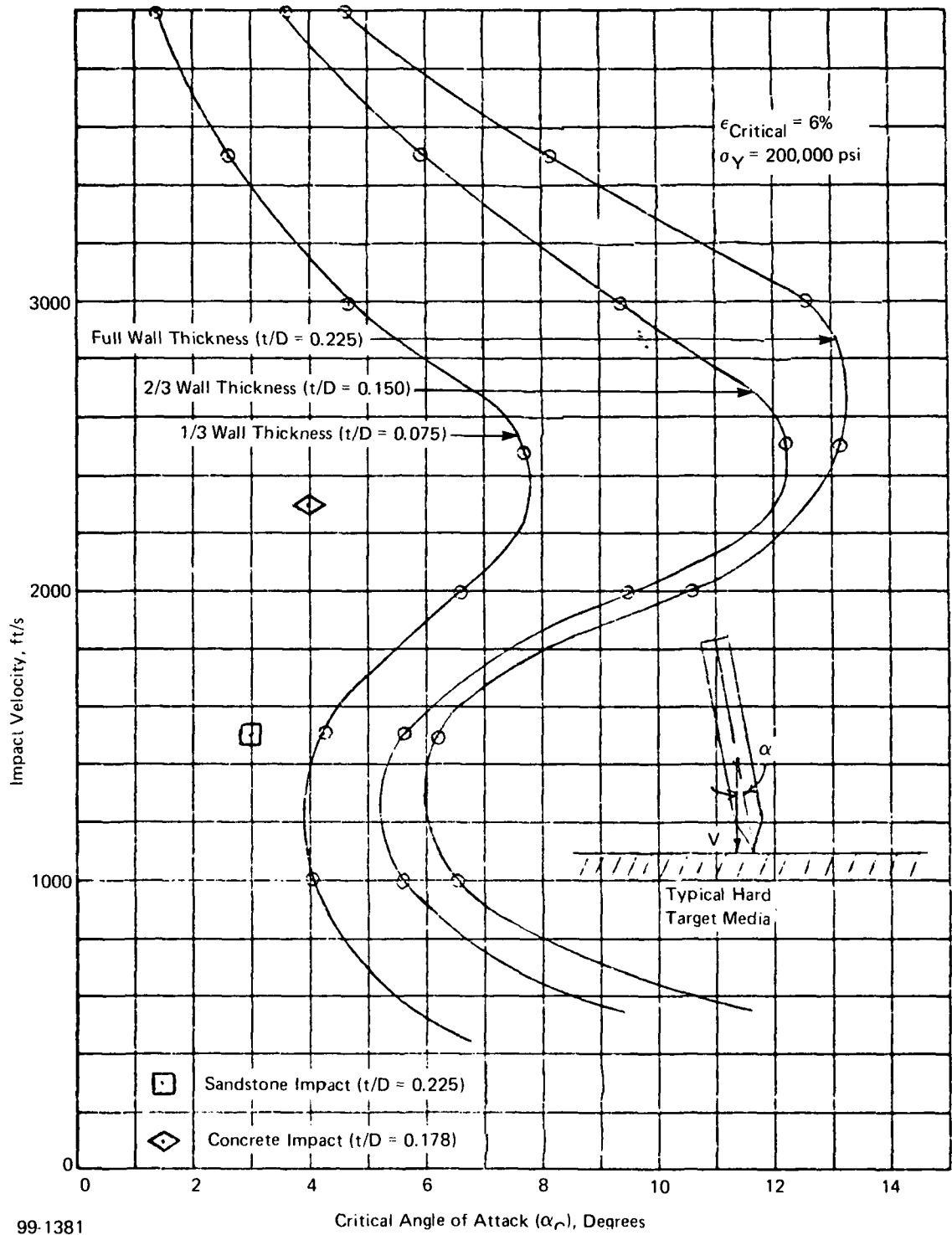
99 1379

Figure 39 Parametric study results - wall thickness - $\epsilon_{\text{critical}} = 2\%$



99-1380

Figure 40 Parametric study results - wall thickness - $\epsilon_{\text{critical}} = 4\%$



99-1381

Figure 41 Parametric study results - wall thickness - $\epsilon_{\text{critical}} = 6\%$

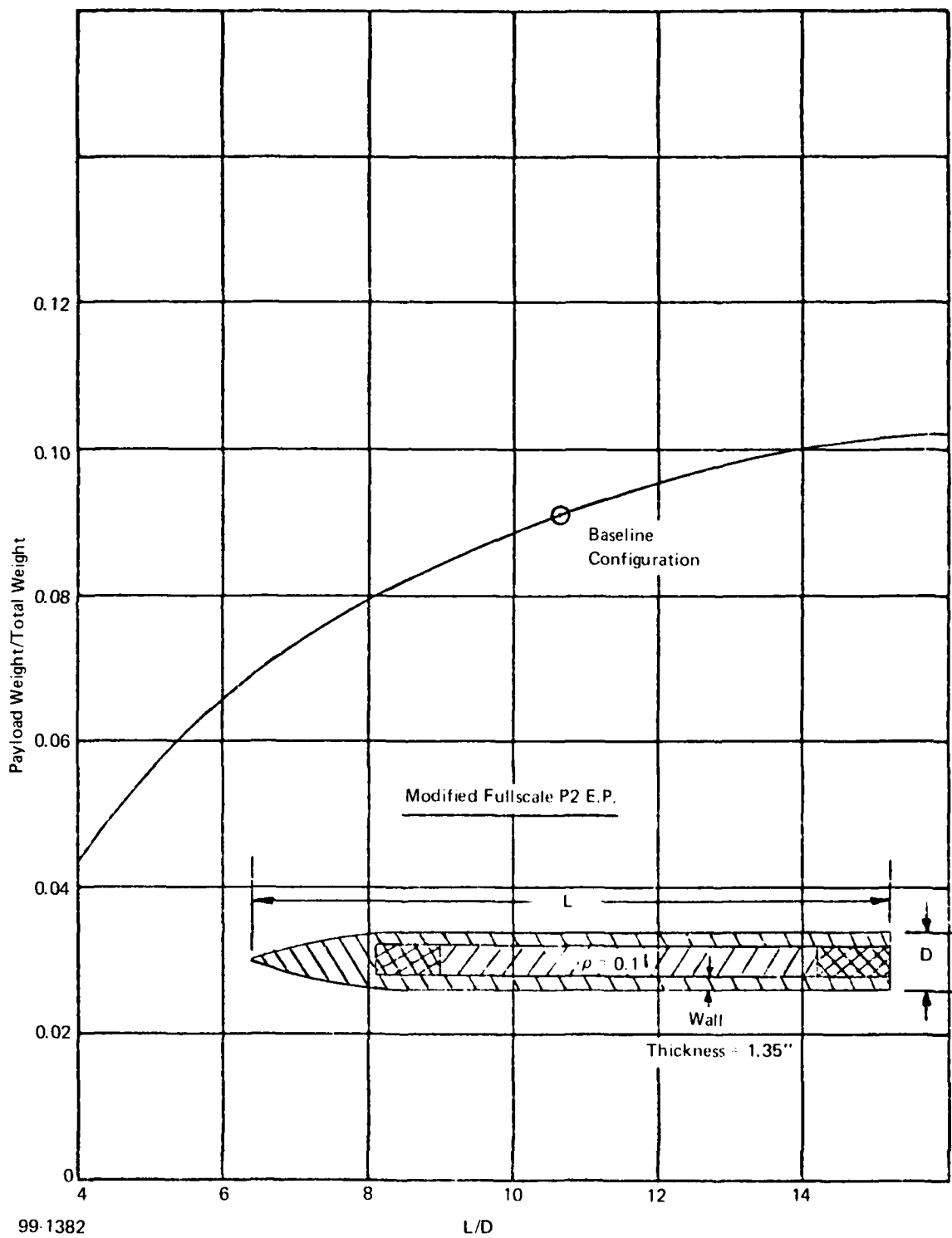
for this study are 6.67, 10 (baseline design), and 15. The same penetrator baseline configuration, material strength, and impact condition ranges were selected. The L/D variations were achieved by increasing or decreasing the penetrator model length while holding the diameter constant. On Figure 42 the payload weight to total weight ratio versus L/D is shown. It is evident from this figure that a low L/D places severe limitations on payload carrying capacity.

The results of the parametric study are presented in Figures 43, 44, and 45. These results indicate several interesting trends regarding penetrator length, response frequency, and impact velocity. For the low L/D (6.67) design it appears that the inflection in the curve occurs below 1000 ft/s. This is because the penetrator achieves full body wetting sooner at lower velocities in relation to its structural response. Thus the results show only the low L/D's response to increasing loading at the higher velocities. For the baseline design (L/D = 10) the results are the same as described previously. The higher L/D (15) design shows an extension of the relationship between impact velocity and structural response frequency. Because of the longer length (and hence longer time to full body wetting) the inflection in the curve occurs at higher velocities. In addition, the L/D = 15 design achieves overall lower critical angles of attack than the baseline design. This is caused by the larger bending moments generated by the longer design which has been fixed to the same diameter as the baseline design. These results indicate that some matching of penetrator L/D to required impact velocities is necessary in order to optimize structural survivability.

Also shown on Figures 43 through 45 are test data points which have been related to the variables under consideration. The test data although sparse does provide limited verification of the analytical model results.

The effect of wall thickness on depth of penetration is shown on Figures 46 and 47 as related to the variables of the previous two parametric studies. Although the penetrator depth is not the prime purpose of this code, it can be used to generate approximate depth of penetration data for system evaluation. These results are self-explanatory and should prove very useful in a design tradeoff study.

These parametric studies have shown the usefulness of the simplified structural analysis procedure. Thus a wide range of geometric, media and impact parameters may be varied efficiently and economically.



99-1382

Figure 42 Penetrator configurations - L/D

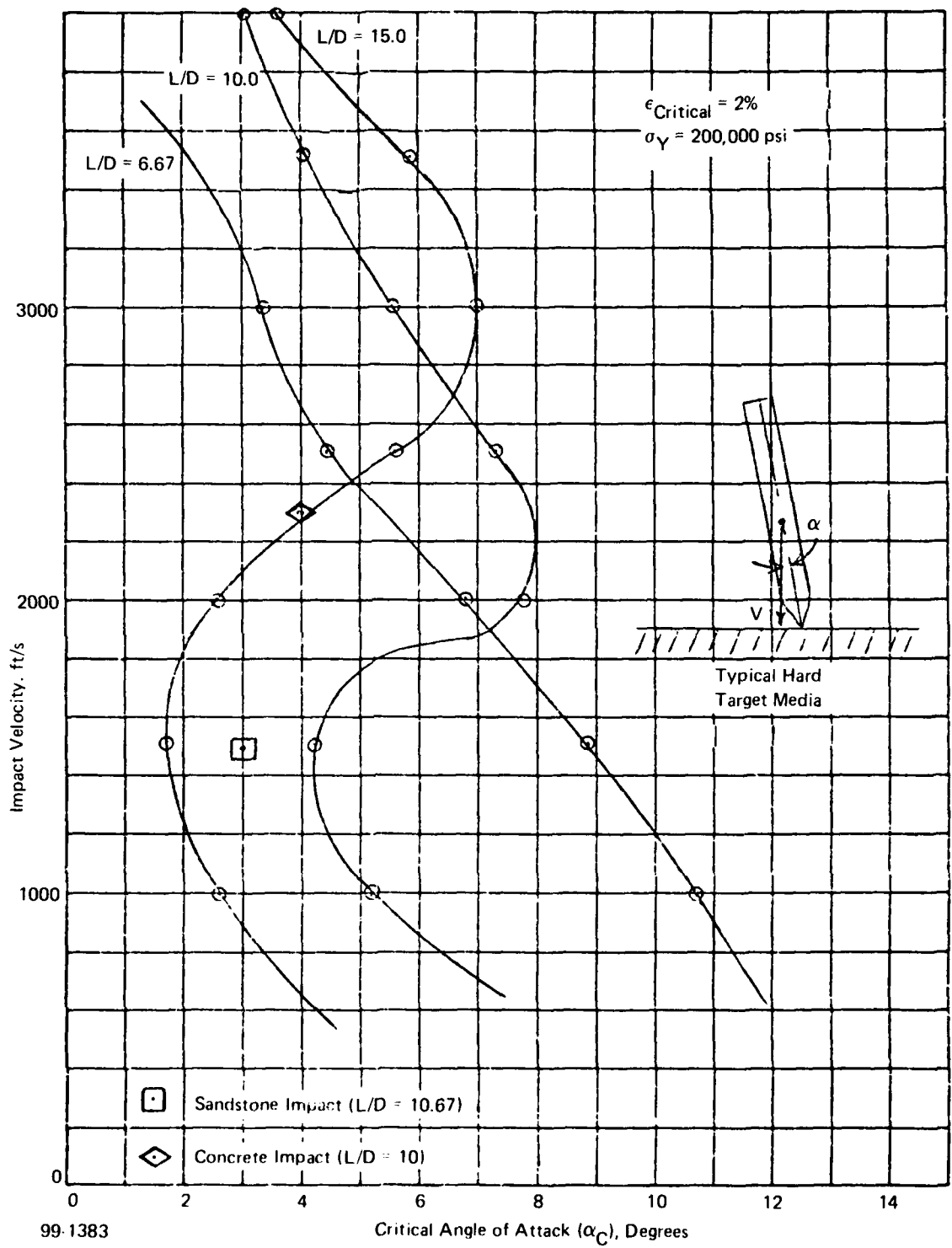
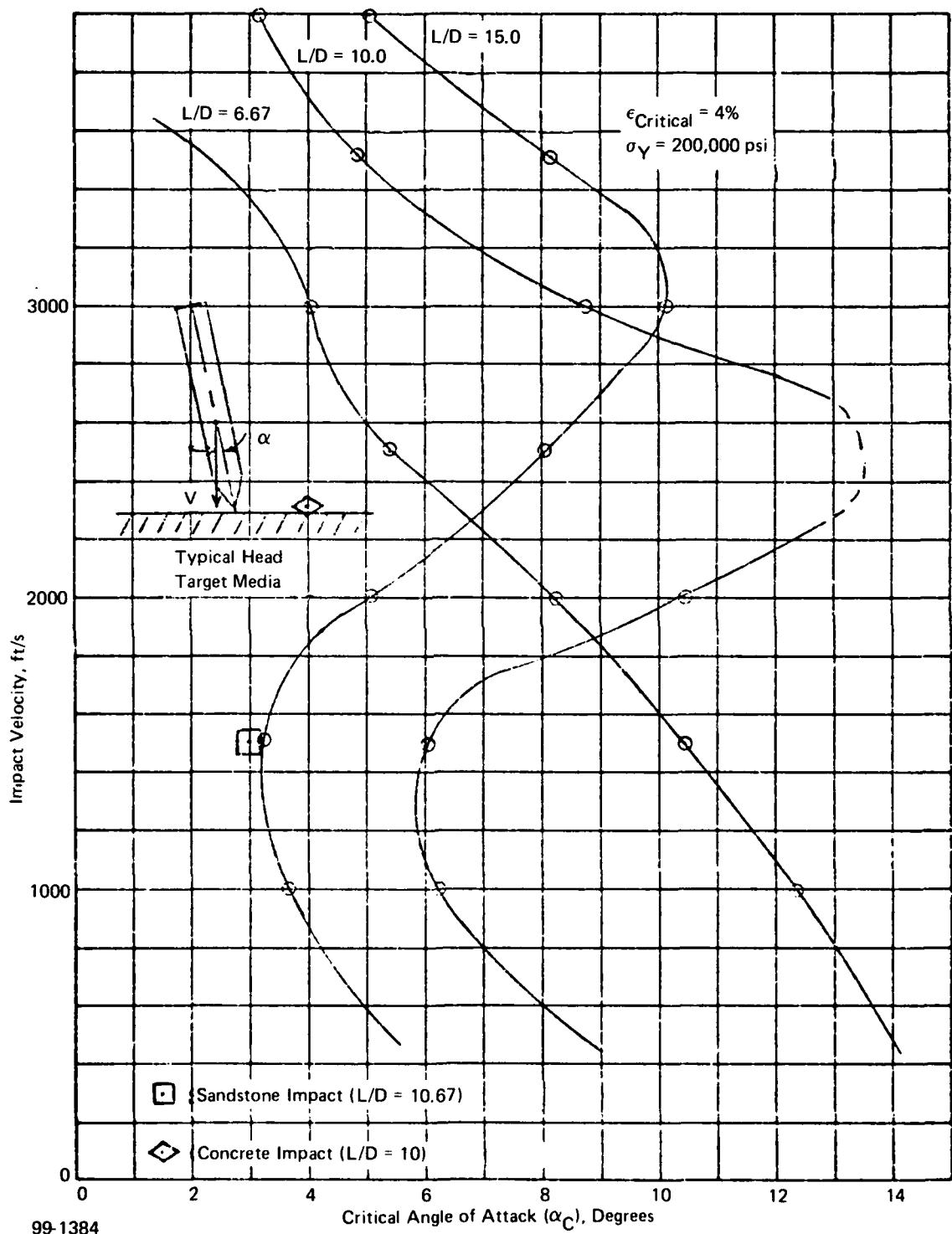
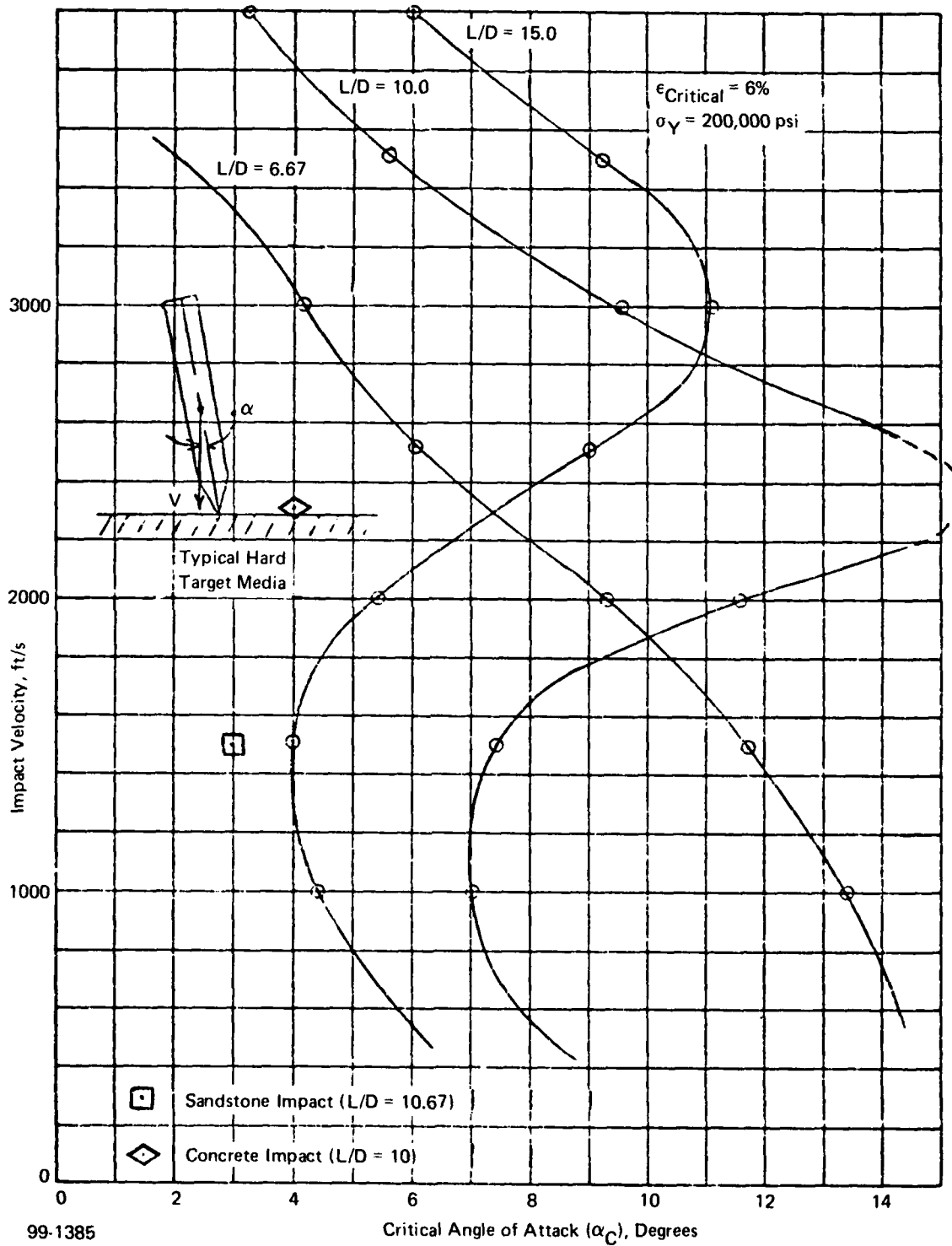


Figure 43 Parametric study results - $L/D - \epsilon_{\text{critical}} = 2\%$



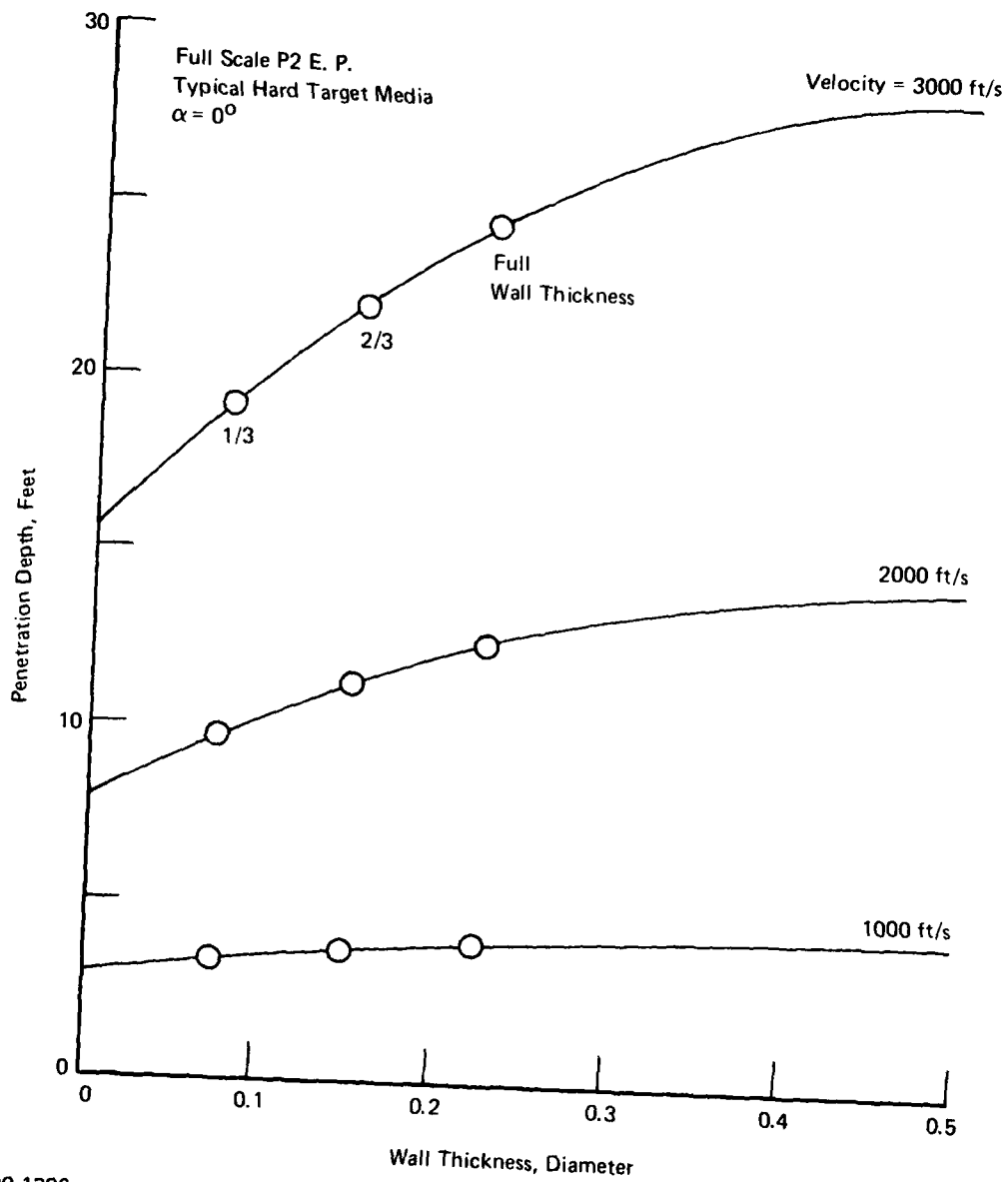
99-1384

Figure 44 Parametric study results - $L/D - \epsilon_{critical} = 4\%$



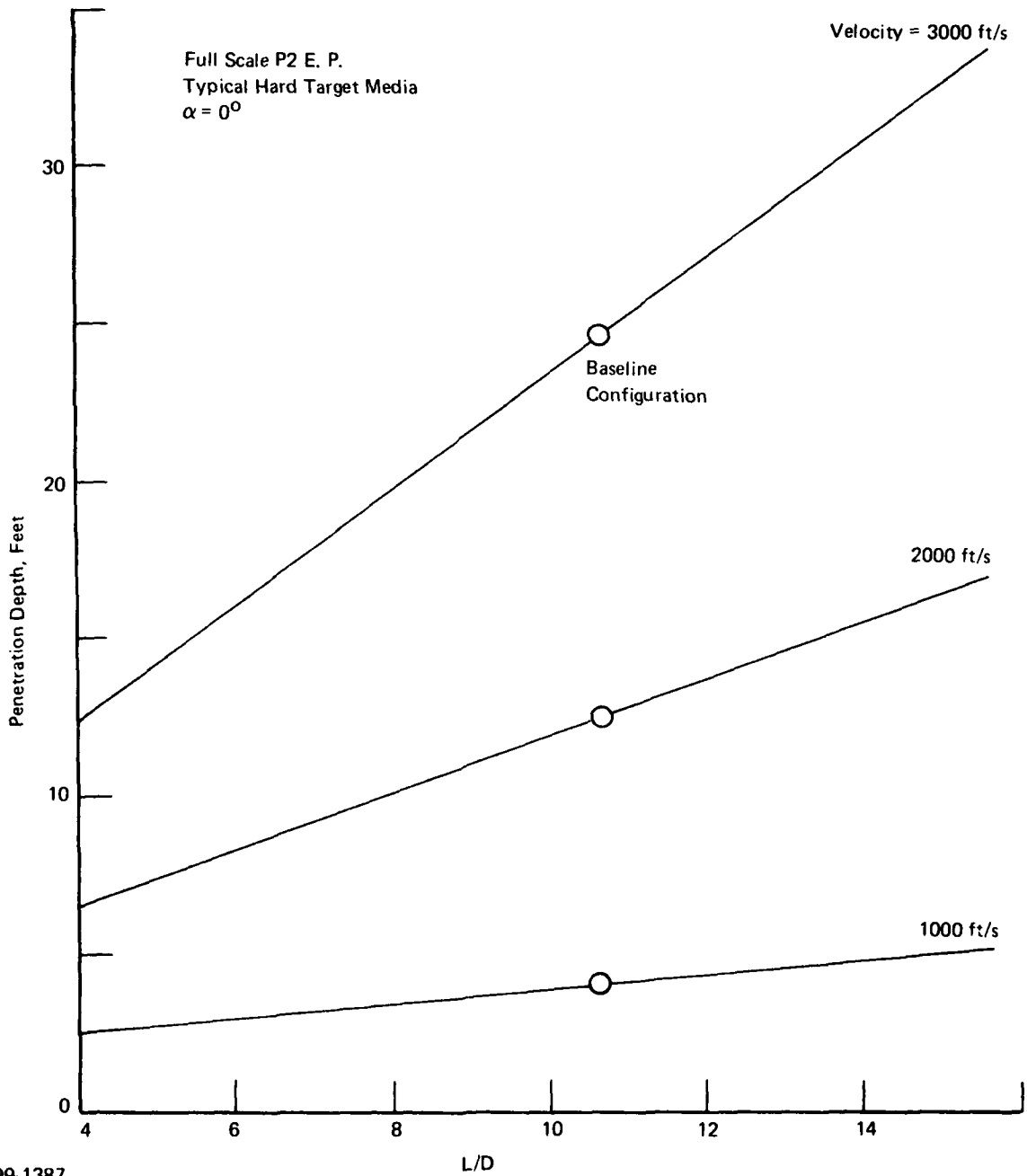
99-1385

Figure 45 Parametric study results - $L/D - \epsilon_{critical} = 6\%$



99-1386

Figure 46 Penetration depth vs. wall thickness



99-1387

Figure 47 Penetration depth vs. L/D

SECTION 7

CONCLUSIONS AND RECOMMENDATIONS

The significant results and conclusions of this program are:

1. A simplified method has been developed and demonstrated.
2. The effects of full body wetting or envelopment were shown to be significant.
3. The structural capability of penetrators can improve with increasing velocity and angle-of-attack.
4. The structural survival penalty for increased payload carrying capacity was found not to be excessive.

The most dramatic of these conclusions is the third one, but as described in the preceding sections, the phenomena is merely a result of the basic resonance phenomena.

The utility of the simplified analytical procedure has been demonstrated by the range of parametric studies indicated and the interesting phenomena identified. The inflection in the capability curves should be further investigated, since the potential for improved penetrator performance has been identified.

As a result of the parametric studies, the following recommendations are made:

1. Perform reverse ballistic diagnostic tests at higher velocities to verify the existence of more favorable impact regimes and to obtain a better definition of the more severe impact loading environments.
2. Perform direct ballistic tests at these higher velocities to define the payoff in penetration performance.
3. Based on the above testing and other test data available, further refine the simplified procedure.

PRECEDING PAGE BLANK-NOT FILMED

REFERENCES

1. Henderson, D., and D. K. Maynard, "Impact and Penetration Technology Program Reverse Ballistic Tests", Contract DNA 001-75-C-0181 Avco Corporation, October 1975.
2. Henderson, D., and E. J. Giara, Jr., "Earth Penetrator Technology Program," Contract DNA 001-77-C-0127 Avco Corporation, January 1978.
3. Dynamics of Structures, Hartly and Rubinstein, 1964.

APPENDIX A

AVCO IMPACT AND PENETRATION TECHNOLOGY PROGRAM SUMMARY

A1.1 TRAJECTORY ANALYSES FY 1975

This effort involved identifying the Impact and Penetration Technology existing at the Avco Systems Division. This capability was used to provide pretest predictions of a full scale impact and penetration event to be conducted by Sandia Laboratories at the "Watching Hill Test Site" in Canada. The trajectory was "straight line" due to the normal impact conditions and excellent correlation was obtained between test results and predictions.

A1.2 AXIAL LOADING AND STRUCTURAL RESPONSE ANALYSES FY 1975

The Avco 16 inch diameter Reverse Ballistic Test Facility* was used to obtain axial structural response of a typical earth penetrator undergoing normal impact events using a concrete media. (See Figure 2.) In support of the tests, pretest predictions were made by several contractors to assess the community's capabilities to predict both the applied loading environments and resulting structural response.

A1.3 OFF NORMAL IMPACT EVENTS FY 1976

This phase also used the Avco Reverse Ballistic Facility to obtain structural response (i.e., strain time history) test data resulting from both normal and angle of attack impact conditions. In this program, six tests were conducted at 1600 ft/sec, for angle of attack ranging from 0 to 10 degrees. A complete description of this program is presented in Reference 1.

A1.4 FULL BODY WETTING INVESTIGATIONS FY 1977

Because of the limited size of the media targets (i.e., 16" diameter x 10" long) used in Avco's reverse ballistic gun tests, only nose wetting (embedment) impact environments could be investigated, but there were indications that nose wetting loads may not be causing peak strain response. It was postulated that the lateral loads may be dominant during or after full body embedment. The FY 77 efforts, therefore, involved reverse ballistic tests using much larger targets. The penetrators were designed, fabricated and instrumented by Avco and subsequently tested by Sandia at their sled test facility. Avco and other contractors made pretest calculations (i.e., predictions) of the event. Avco used its differential force law technique to predict the loads for use in a lumped parameter axial/lateral beam model which represented the penetrator structure. The Avco pretest predictions indicated excellent agreement with test results. This effort is documented in Reference 2. As a result of this program, it was still not established whether full body lateral loads were critical from a structural survival point of view.

* The target media is impacted into a static instrumented penetrator.

This was not established until the current program where it was determined that full body loading is one of the critical design conditions for high L/D penetrators. The analytical technique described in Section 5.0 allows for a direct comparison between nose wetting (embedment) and full body wetting.

DISTRIBUTION LIST

DEPARTMENT OF DEFENSE

Assistant to the Secretary of Defense
Atomic Energy
ATTN: Executive Assistant

Defense Advanced Rsch. Proj. Agency
ATTN: T10

Defense Intelligence Agency
ATTN: DB-4N
ATTN: RDS-3A
ATTN: DB-4C, E. O'Farrell
ATTN: DT-2

Defense Nuclear Agency
ATTN: SPAS
ATTN: DDST
ATTN: STSP
4 cy ATTN: TITL
5 cy ATTN: SPSS

Defense Technical Information Center
12 cy ATTN: DD

Federal Emergency Management Agency
ATTN: Hazard Eval. & Vul. Red. Div., G. Sisson

Field Command
Defense Nuclear Agency
ATTN: FCPR

Field Command
Defense Nuclear Agency
Livermore Division
ATTN: FCPRL

Interservice Nuclear Weapons School
ATTN: TTV

Joint Strat. Tgt. Planning Staff
ATTN: NRL-STINFO Library

NATO School (SHAPE)
ATTN: U.S. Documents Officer

Undersecretary of Defense for Rsch. & Engrg.
ATTN: Strategic & Space Systems (OS)

DEPARTMENT OF THE ARMY

Chief of Engineers
Department of the Army
2 cy ATTN: DAEN-RDM
2 cy ATTN: DAEN-MCE-D

Deputy Chief of Staff for Ops. & Plans
Department of the Army
ATTN: DAMO-NC
ATTN: MOCA-ADL

Deputy Chief of Staff for Rsch., Dev., & Acq.
Department of the Army
ATTN: DAMA-CSS-N, N. Barron

Engineer Studies Center
Department of the Army
ATTN: DAEN-FES

DEPARTMENT OF THE ARMY (Continued)

Gator Mine Program
Department of the Army
ATTN: E. Lindsey

Harry Diamond Laboratories
Department of the Army
ATTN: DELHD-N-P, J. Gwaltney
ATTN: DELHD-N-P

U.S. Army Armament Material Readiness Command
ATTN: MA Library

U.S. Army Ballistic Research Labs.
ATTN: DRDAR-BLT
ATTN: DRDAR-BLT, A. Ricchiuzzi
ATTN: DRDAR-BLT, G. Roecker
ATTN: DRDAR-BLT, G. Grabarek
ATTN: DRDAR-BLE, J. Keefer
ATTN: DRDAR-BL
2 cy ATTN: DRDAR-TSB-S

U.S. Army Cold Region Res. Engr. Lab.
ATTN: G. Swinzow

U.S. Army Engineer Center
ATTN: AT2A

U.S. Army Engineer Div., Huntsville
ATTN: HNEED-SR

U.S. Army Engineer Div., Missouri River
ATTN: Technical Library

U.S. Army Engineer School
ATTN: AT2A-CDC
ATTN: AT2A-DTE-ADM

U.S. Army Engr. Waterways Exper. Station
ATTN: B. Rohani
ATTN: WESSE, L. Ingram
ATTN: Library
ATTN: WESSA, W. Flathau
ATTN: WESSD, G. Jackson
ATTN: J. Strange
ATTN: D. Butler

U.S. Army Mat. Cmd. Proj. Mngr. for Nuc. Munitions
ATTN: DRCPM-NUC

U.S. Army Material & Mechanics Rsch. Ctr.
ATTN: Technical Library

U.S. Army Materiel Dev. & Readiness Cmd.
ATTN: DRXAM-TL

U.S. Army Materiel Sys. Analysis Activity
ATTN: DRASY-D, J. Sperrazza

U.S. Army Missile Command
ATTN: F. Fleming
ATTN: RSIC
ATTN: DRCPM-PE, W. Jann

U.S. Army Mobility Equip. R&D Cmd.
ATTN: DRDME-WC
ATTN: DRDDME-XS

DEPARTMENT OF THE ARMY (Continued)

U.S. Army Nuclear & Chemical Agency
ATTN: Library

U.S. Army War College
ATTN: Library

DEPARTMENT OF THE NAVY

Marine Corps
Department of the Navy
ATTN: POM

Marine Corp Dev. & Education Command
Department of the Navy
ATTN: D091, J. Hartneady

Naval Air Systems Command
ATTN: F. Marquardt

Naval Construction Battalion Center
ATTN: Code L0SA
ATTN: Code L51, R Odello

Naval Explosive Ord. Disposal Fac.
ATTN: Code 504, J. Petrusky

Naval Facilities Engineering Command
ATTN: Code O9M22C

Naval Postgraduate School
ATTN: Code 0142 Library

Naval Research Laboratory
ATTN: Code 2627

Naval Sea Systems Command
ATTN: SEA-9931G
ATTN: SEA-033

Naval Surface Weapons Center
ATTN: Code X211
ATTN: Code F31
ATTN: Code U401, M. Kleinerman

Naval Surface Weapons Center
ATTN: Tech. Library & Info. Services-Branch

Naval weapons Center
ATTN: Code 233
ATTN: Code 266, C. Austin

Naval Weapons Evaluation Facility
ATTN: Code 10

Office of Naval Research
ATTN: Code 715

Office of the Chief of Naval Operations
ATTN: OP 982E, M. Lenzini
ATTN: OP 604C3, R. Piacesi
ATTN: OP 982

Strategic Systems Project Office
Department of the Navy
ATTN: NSP-43

DEPARTMENT OF THE AIR FORCE

Air Force Institute of Technology
ATTN: Library

DEPARTMENT OF THE AIR FORCE (Continued)

Air Force Armament Laboratory
ATTN: ADTC/XRS, M. Valentine
3 cy ATTN: DLYV, J. Collins

Air Force Weapons Laboratory
Air Force Systems Command
ATTN: SUL

Assistant Chief of Staff, Intelligence
Department of the Air Force
ATTN: INT

Deputy Chief of Staff
Research, Development, & Acq.
Department of the Air Force
ATTN: R. Steere

Foreign Technology Division
Air Force Systems Command
ATTN: NIIS Library

Headquarters Space Division
Air Force Systems Command
ATTN: RSS

Oklahoma State University
Fld. Office for Wpns Effectiveness
Department of the Air Force
ATTN: E. Jackett

Rome Air Development Center
Air Force Systems Command
ATTN: TSLD

DEPARTMENT OF ENERGY

Department of Energy
Albuquerque Operations Office
ATTN: CTID

Department of Energy
ATTN: Document Control for OMA/RD&T

Department of Energy
Nevada Operations Office
ATTN: Mail & Records for Technical Library

DEPARTMENT OF ENERGY CONTRACTORS

Lawrence Livermore Laboratory
ATTN: Document Control for L-504, M. Wilkins
ATTN: Document Control for J. Goudreau
ATTN: Document Control for Tech. Info. Dept. Lib.

Los Alamos Scientific Laboratory
ATTN: Document Control for MS 364
ATTN: Document Control for M/5632, T. Dowler

Sandia Laboratories
ATTN: Document Control for W. Herrmann
ATTN: Document Control for 3141
ATTN: Document Control for W. Patterson
ATTN: Document Control for A. Chahai
ATTN: Document Control for W. Altsmeirer
ATTN: Document Control for W. Caudle
ATTN: Document Control for J. Kaizur
ATTN: Document Control for J. Colp

DEPARTMENT OF ENERGY CONTRACTORS (Continued)

Sandia Laboratories
Livermore Laboratory
ATTN: Document Control for Library & Security
Classification Division

OTHER GOVERNMENT AGENCIES

NASA
ATTN: R. Jackson

U.S. Nuclear Regulatory Commission
ATTN: Div. Of Security for L. Shao

DEPARTMENT OF DEFENSE CONTRACTORS

Aerospace Corp.
ATTN: Technical Information Services

Agbabian Associates
ATTN: M. Agbabian

Applied Theory, Inc.
2 cy ATTN: J. Trulio

AVCO Research & Systems Group
ATTN: P. Grady
ATTN: D. Henderson
ATTN: Library A830

BDM Corp.
ATTN: Corporate Library
ATTN: T. Neighbors

Boeing Co.
ATTN: Aerospace Library

California Research & Technology, Inc.
ATTN: K. Kreyenhagen
ATTN: Library
ATTN: M. Ito

California Research & Technology, Inc.
ATTN: D. Orphal

Civil Systems, Inc.
ATTN: J. Bratton

EG&G Washington Analytical Services Center, Inc.
ATTN: Library

Engineering Societies Library
ATTN: A. Mott

General Dynamics Corp.
ATTN: K. Anderson

General Electric Company—TEMPO
ATTN: DASIAC

Honeywell, Inc.
ATTN: T. Helvig

University of Illinois, Consulting Services
ATTN: W. Hall
ATTN: N. Newmark

TRW Defense Analyses
ATTN: Classified Library

DEPARTMENT OF DEFENSE CONTRACTORS (Continued)

Kaman Avidyne
ATTN: Library
ATTN: N. Hobbs
ATTN: E. Criscione

Kaman Sciences Corp.
ATTN: Library

Lockheed Missiles & Space Co., Inc.
ATTN: Technical Information Center

Lockheed Missiles & Space Co., Inc.
ATTN: TIC-Library
ATTN: M. Culp

Martin Marietta Corp.
ATTN: A. Cowan
ATTN: M. Anthony
ATTN: H. McQuaig

Merritt CASES, Inc.
ATTN: Library
ATTN: J. Merritt

University of New Mexico
ATTN: G. Triandafalidis

Pacific-Sierra Research Corp.
ATTN: H. Brode

Pacifica Technology
ATTN: G. Kent
ATTN: R. Bjork

Physics International Co.
ATTN: L. Behrmann
ATTN: Technical Library

R & D Associates
ATTN: W. Wright, Jr.
ATTN: C. MacDonald
ATTN: J. Lewis
ATTN: A. Field
ATTN: P. Rausch
ATTN: Technical Information Center

R & D Associates
ATTN: H. Cooper

Rand Corp.
ATTN: Library

Science Applications, Inc.
ATTN: Technical Library

SRI International
ATTN: J. Colton
ATTN: G. Abrahamson

Systems, Science & Software, Inc.
ATTN: Library
ATTN: R. Sedgewick

Terra Tek, Inc.
ATTN: Library

TRW Defense & Space Sys. Group
ATTN: P. Dai
ATTN: Technical Information Center

DEPARTMENT OF DEFENSE CONTRACTORS (Continued)

TRW Defense & Space Sys. Group
ATTN: E. Wong

Weidlinger Assoc., Consulting Engineers
ATTN: J. Isenberg

DEPARTMENT OF DEFENSE CONTRACTORS (Continued)

Weidlinger Assoc., Consulting Engineers
ATTN: M. Baron
ATTN: J. McCormick

DATE
FILMED
8-8